University of
South-Eastern Norway

www.usn.no

FMH606 Master's Thesis 2018
Electrical Power Engineering

Frequency stability in integrated synchronous power systems

Sigrid Lauvik Lyngdal

Faculty of Technology, Natural sciences and Maritime Sciences
Campus Porsgrunn

University of South-Eastern Norway

www.usn.no

Course: FMH606 Master's Thesis, 2018

Title: Frequency stability in integrated synchronous power systems

Number of pages: 86

Keywords: Frequency stability, Nordic synchronous power system, turbine governor, FCR, FCR-D, FCR-N

Student: Sigrid Lauvik Lyngdal

Supervisor: Gunne John Hegglid

External partner: -

Availability: Open

Summary:

In the later years, the frequency quality in the Nordic synchronous system has been reduced significantly. In order to restore the frequency quality, new requirements for the primary frequency control (FCR) is under development by the Nordic TSOs. The new FCR requirements based on stability and dynamic performance have been tested for a single unit in Sundsbarm power plant and for a single unit in Hjartdøla power plant. Simulation models was build up to mirror the behaviour of the power plants during the tests. The new stability requirentent for syncronous operation is similary to the FIKS stabiltiy requiremnt for seperat operation. However, the 'system' that regulates against is different. It is desired that the providing unit should deliver steady-state power within 5 seconds at disturbances. Results from the tests, showns that the hydropower units fullfil the stability requirements. The tests expose also that the hydropower units can deliver 100% steady-state power response within 5 seconds. Except for the unit in Hjartdøla power plant tested with 4% droop setting which can deliver 91% of full steady-state response at downwards regulation.

Preface

This master's thesis was written during the spring 2018 as a graduation on my degree Master of Science in Electrical Power Engineering at the University of Southeast Norway (USN). It has been a very educational and exciting process and I hope Skagerak Kraft AS will has benefited from the results in this thesis.

I would like to thank my supervisor Gunne John Hegglid for all the knowledge he has shared with me and his guidelines through the work of this thesis. I would also like to thank Dietmar Winkler at the USN for helping me with the simulations models in the software Dymola.

Porsgrunn, 15.05.2018

Sigrid Lauvik Lyngdal

Contents

Nomenclature

Abbreviations

aFRR	Automatic Frequency Restoration Reserve
ENTSO-E	European Network of Transmission System Operators for Electricity
FCR	Frequency Containment Reserve
FCR-D	Frequency Containment Reserve for Disturbance
FCR-N	Frequency Containment Reserve for Normal operation
FIKS	Funksjonskrav i kraftsystemet
mFRR	Manual Frequency Restoration Reserve
TSO	Transmission System Operator

1 Introduction

1.1 Background

In the later years, it is registered that the frequency oscillations in the Nordic synchronous power system have a significant impact on the frequency quality. The oscillations are a result of imbalances between power production and consumption in the system. The amount of inertia and reserves in the system is important for balancing process. The development with more production from wind, solar and small hydro contributes marginally to inertia in the system and hence reducing the frequency quality. In order to increase the frequency quality in the Nordic synchronous system, the project “Revision of the Nordic Frequency Containment Project” (FCP-project) was started up at the end of 2014 to create new technical requirements for primary frequency control.

In order to participate in the primary control markets, the hydropower units have to be prequalified according to the new technical requirements. The prequalification process including a set of prequalification tests to determine the stability and dynamic performance of the units.

1.2 Objectives

- Describe the balancing of the Nordic synchronous power system
- Review of the existing requirements from FIKS – “Funksjonskrav i kraftsystemet” weight on the turbine governor and stability requirement.
- Perform the prequalification tests of two hydropower units owned by Skagerak Kraft As with the current governor settings. The tests should be performed for a single unit in Sundsbarm power plant and for a single unit in Hjartdøla power plant.
- Build up simulation models for Sundsbarm and Hjartdøla power plants in order to test stability and dynamic performance of the hydropower units according to the new FCR requirements

1.3 Report structure

The thesis is organized into nine chapters. Chapter 1 describes balancing of the Nordic synchronous system, including primary frequency control, secondary frequency control and tertiary frequency control. Chapter 2 is theory about waterway, hydropower unit and governing system with focus on stability and existing requirements. In chapter 3, the new FCR-N and FCR-D requirements and test procedure for verifying the requirements are outlined. Chapter 4 describes the software used and the simulation models with obtained parameters for Sundsbarm and Hjartdøla power plants. In chapter 5, tuning and testing of the turbine governor is outlined. Chapter 7 is a presentation and analysis of the simulation results for verifying the FCR-N/D requirements. Discussion on the simulation model, stability and performance are presented in chapter 8, and the conclusions are drawn in chapter 9.

2 Balancing of the Nordic synchronous system

The frequency is an indicator of the power system's ability to handle imbalances in normal operation and disturbances. The Nordic region with Finland, Sweden, Sealand of Denmark and Norway is a synchronous system with a common frequency at 50.00 Hz. Any imbalances anywhere in the system will thus affect the common frequency of the system. The requirement for a normal frequency band is specified at 50.0 Hz +/- 0.1 Hz. The TSO of each of the countries are responsible for system balancing within each country.

A critical task in the operation of the Nordic synchronous system is to maintain the power balance between the production and the consumption in an economically optimal way every minute of the day, night, week and year. When a power system is exposed to a power imbalance e.g. by tipping of a generating unit or if a large load is suddenly connected or disconnected to the system, there will be a long-term distortion in the power balance between delivered and consumed power. The power imbalances will lead to frequency variations from the nominal value, 50.00 Hz. So, if the consumption is higher than the delivering of power, the frequency decrease, and if the delivering is higher than the consumption, the frequency increase. The greater the frequency deviation and the longer the frequency is outside the band, the greater the risk of major negative consequences in the event of a major production loss.

The frequency is continuously influenced by the rotating mass in the system and activation of frequency control reserves. The frequency controls in the Nordic power market are the primary control, using Frequency Containment Reserves (FCR), the secondary control, using the Automatic Frequency Restoration Reserves (aFRR) and the tertiary control, using Manual Frequency Restoration Reserves (mFRR).

The response of a power system when a power imbalance occurs can be divided into four stages depending on the duration of the dynamics involved [1]:

Stage I: Rotor swings in the generators

Stage II: Frequency change (0-5 s)

Stage III: Primary control by the turbine governing systems (5-30 s)

Stage IV: Secondary control by the central regulators (30 s-15 min)

After the secondary control, stage IV, the tertiary control will be activated. Figure 2.1 shows how the frequency controls respond when a frequency deviation occurs.

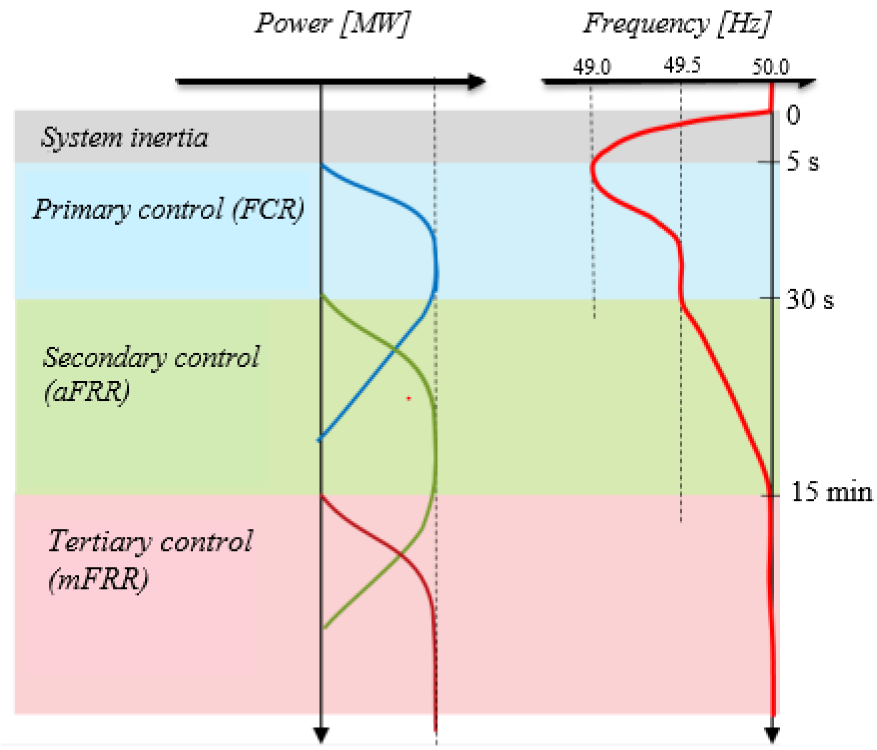

Figure 2.1: Response of a power system

If a hydropower unit is disconnected due to for instance a fault, neighboring hydropower units will initially produce large rotor swings and the other hydropower units within the system will produce much smaller rotor swings. This is stage I of the response in a power system. Stage II is the frequency drop, shown in the right curve in Figure 2.1. How fast the frequency drops depend on the amount of rotating mass (inertia) in the system. Stage III is when the primary control (FCR) is activated to stabilize the frequency. The primary control is automatically activated when the frequency starts to drop. Within minutes the secondary control (aFRR) will be activated to bring back the frequency close to 50.00 Hz and release the primary control.

For additional frequency control, the tertiary control (mFRR) is activated and release the secondary control. Tertiary control is manually activated by the TSOs [1, 2]. A more thorough explanation of the controls is presented in the following subsections.

2.1 Inertia

The inertia of a power system is the ability of a system to oppose changes in frequency due to the resistance provided by kinetic energy of the rotating masses in synchronous machines. In case of major operational disturbances, low inertia in the system causes an increased risk of disconnection of consumption due to low frequency. The system inertia is most important for limiting the frequency drop and stabilizing the system for the first few seconds after a disturbance, before the primary control responds. Too low inertia can cause the frequency drop to such a low level that consumption is eliminated, and at worst case, a larger area becomes darkened [3] [4].

The inertia constant indicates how much rotational mass a hydropower unit contributes to the system, and can be interpreted as the time that energy stored in rotating parts of a machine is able to supply a load equal to its rated apparent power [3]:

$$H = \frac{1}{2}\frac{J\omega_m^2}{S_n} \tag{2.1}$$

Where

H Inertia constant $[s]$

J Moment of inertia $[kgm^2]$

ω_m Mechanical angular frequency $[rad/s]$

S_n Rated apparent power $[VA]$

Figure 2.2 shows how the inertia constant varies for different types of production units. Nuclear and thermal power plants have the largest inertia constants. The units are rotating fast because of the low mass, while hydropower units are rotating slowly because of relative large mass. The inertia constant for HVDC and wind power is zero and do not provide inertia to the power system.

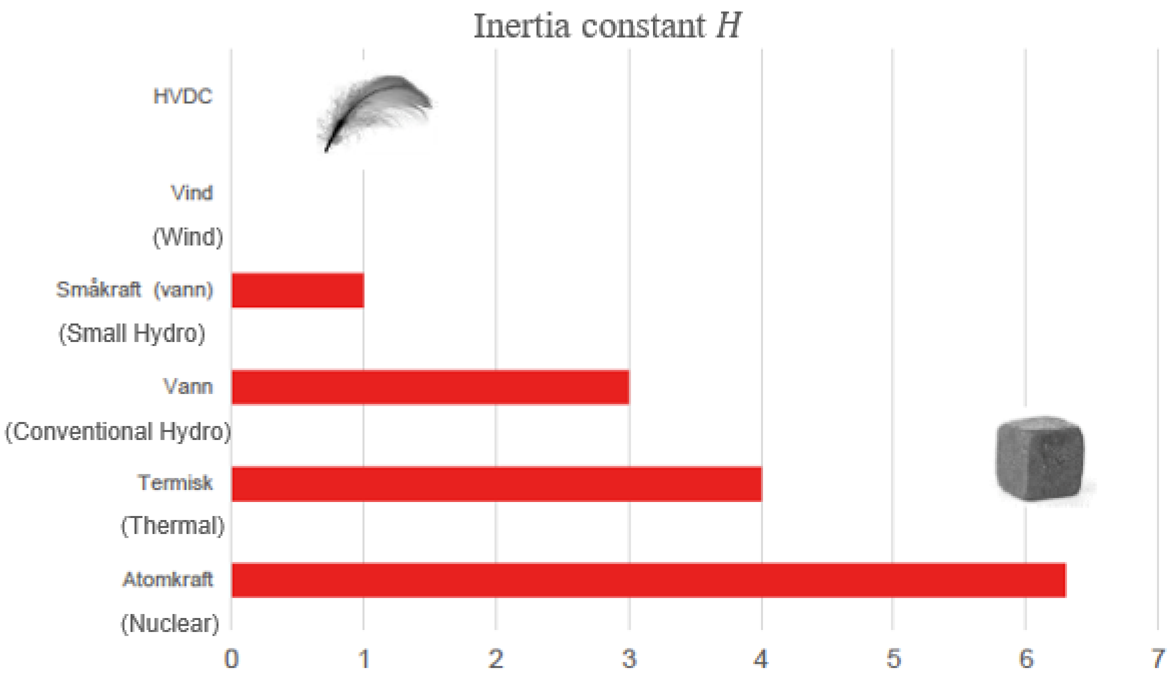

Figure 2.2: Inertia constants used by Statnett [5]

The Nordic synchronous system has historically had a relatively stable continuous operation of large hydropower and nuclear power plants. However, current trends with more wind power production, more use of HVDC-cables and less nuclear power production leads to less inertia in the power system.

2.2 Primary Frequency Control

The primary frequency control in the Nordic synchronous system is called the Frequency Containment Reserve (FCR). The objective of the primary frequency control is to maintain the balance between production and consumption. A change in the power balance changes the kinetic energy of the rotation mass of the unit and alters the system frequency. The primary control stabilizes the system frequency at a stationary value by using a so-called turbine governor when an imbalance in the power system occurs [6]. The governor sets with a frequency-power characteristic called droop [7]. The primary control has activation time up to 30 seconds [6].

The Nordic FCR has two different products, one for disturbances (FCR-D) and one for normal operations (FCR-N). The FCR-N is automatically activated when the frequency varies between 50.10 Hz and 49.90 Hz. The FCR-D is automatically activated when frequency drops below 49.90 Hz or over 50.10 Hz. It is a requirement that stationary frequency should not drop below 49.50 Hz in the Nordic power system, and at a higher frequency than this must all the FCR-D must be activated [8].

A separate market is established to ensure that there is sufficient primary response in the system. The primary control market consists of a weekly and a 24-hour market [6].

2.3 Secondary Frequency Control

The objective of the secondary control (Automatic Frequency Restoration Reserve, aFRR) is to restore the system frequency back to the nominal value and releasing the primary control. Secondary control is also referred as Load Frequency Control (LFC) [9].

The secondary control activates when the TSO send a control signal to the power supplier's control system, which automatically changes the power production or consumption of the unit. The secondary control is handled by the Automatic Generation Controller (AGC). AGC transfers the set-point to the generator automatically when the controller receives control orders from the TSO. The response time for the secondary control is approximately 120-210 seconds after the AGC received the signal from the TSO [9].

2.4 Tertiary Frequency Control

The tertiary control (Manual Frequency Restoration Reserve, mFRR) is used to regulate the imbalances in the power systems and release the primary- and secondary control, but also to handle regional bottlenecks. Tertiary control is a common denomination of manual reserves that have an activation time of up to 15 minutes. All the countries in the Nordic synchronous system are required to have tertiary control reserves equal to the dimensional fault for the subsystem [10].

There is a common balancing market for the Nordic power system, called Regulating Power Market (RPM). The power producers and consumers bid a certain amount of power to a specified price in the RPM. The bids are placed in a common Nordic list and are activated based on price order so that the cheapest bid is activated first if there is a need for tertiary control [10].

2.5 From ACE to MACE

The traditional frequency control in the Nordic power system is Area Control Error (ACE). The ACE estimate the imbalances remaining after the primary control and interchange. The future balancing model for the Nordic power system is to comb the frequency control with modern IT-system, called Modern Area Control Error (MACE) [11].

2.5.1 ACE – Area Control Error

The Area Control Error is a measure of the surplus or the lacking amount of power in an area of the power system. The ACE can be calculated per country or per bidding zone. A negative ACE indicates that the area generates too little power to exchange the scheduled amount. A positive ACE means that the area produces excess power and exchanges more than the scheduled amount. The sum of the ACE in a synchronous area must be zero in order to get a balanced power system at the nominal frequency. A frequency deviation occurs if the sum of all the calculated ACE is different from zero [11, 12].

Today, the ACE is balanced on a Nordic level, shown in Figure 2.3. This entails more challenges to control the Nordic frequency and makes it hard to identify costs per country in balancing activities [13].

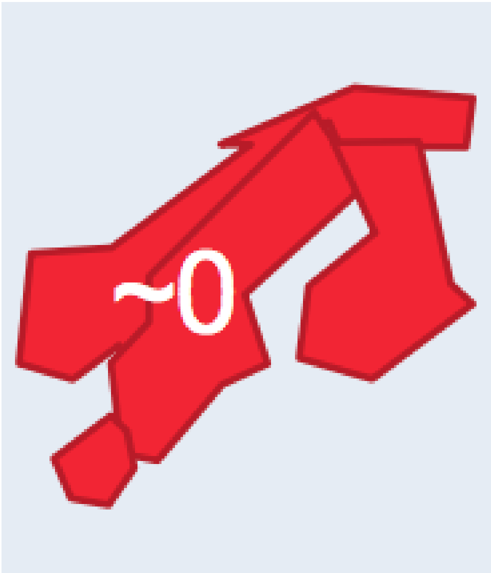

Figure 2.3: Today – Frequency balancing on a Nordic level

2.5.2 MACE – Modern Area Control Error

The purpose of MACE is to use modern IT technology to improve the coordination and optimize the balancing in the Nordic power system. The Nordic power system is divided into different bidding zones, where the main bottlenecks in the grid divide the zones, shown in Figure 2.4. This means that each bidding zone is balanced according to their individual ACE. The MACE will improve the imbalances per bidding zone, and better the harmonization with the rest of Europe [11, 13].

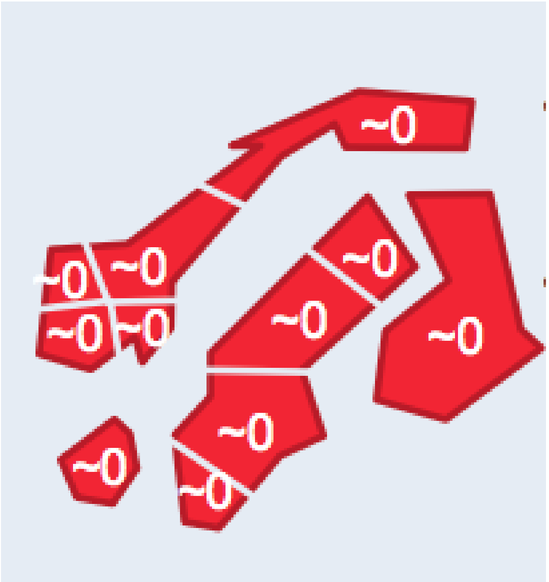

Figure 2.4: Future – the balancing of ACE with modern IT solutions

An important part of using MACE to balance the Nordic power system is coordinating the aFRR and mFRR in all the bidding zones. The MACE controller calculates or decides the desired reserve activation in each of the 11 bidding zones. By using a central optimization function, that indicates the needs for activation in all regions, will the controller find the cheapest bidding zone to be activated [11].

3 Hydropower components

This chapter explained the functionality and existed requirements for the waterway, the hydropower unit and the governing system when the power plant participates in frequency control.

3.1 Waterway

It is important that the waterway is dimensioned to provide system stability when the power plant participates in frequency control. Two aspects of the dynamics in the waterway are especially considered; pressure in front of the turbine and mass oscillations.

3.1.1 Pressure in front of the turbine

When the water flow in the penstock changes due to changing the turbine opening, the water masses in the penstock are accelerating or retardation. Hence, the pressure in front of the turbine changes. The pressure front propagates upward in the penstock with the speed of sound [14].

The pressure surge can be estimated in two ways, by considering the water and pipe either as inelastic or elastic. Inelastic water and pipe will in practice correspond to an infinite speed of sound. When the penstock is long, it has been shown that the elasticity effect must be taken into account [14]. In worst case, by assuming inelastic behaviour the pressure in front of the turbine can be doubled in relation to consider elastic behaviour.

The elasticity of the water and pipe causes water hammer in front of the turbine which their magnitude may be much larger than the nominal pressure in the waterway. The time the pressure wave uses from the turbine and up to the nearest free surface upwards and back again is [14]:

$$T_r = \frac{2L}{a} \tag{3.1}$$

Where

T_r	Reflection time $[s]$
L	Length of the pipe $[m]$
a	Speed of sound ≈ 1200 $[m/s]$

The pressure rise is dependent of the valve closing time (from fully open to close) T_L.

If $T_L < T_r$, the pressure rise is independent of T_L [14]:

$$\Delta h = \frac{\Delta c \cdot a}{g} \tag{3.2}$$

By setting

$$\Delta c = \frac{\Delta Q}{A_p} \tag{3.3}$$

Where

Δh	Pressure rise $[m]$
Δc	Velocity $[m/s]$
ΔQ	Change in flow rate $[m^3/s]$
A_p	Cross-section of the pipe $[m^2]$

A rough estimate, if $T_L > T_r$ the pressure rise is [14]:

$$\Delta h = \frac{\Delta c \cdot a}{g} \left(\frac{T_r}{T_L}\right) \tag{3.4}$$

The pressure rise is greatest when the change in flow rate is greatest. Therefore, the maximum water hammer occurs when closing the turbine. A surge tank is often placed in the waterway to reduce the water hammer [14].

3.1.2 Mass oscillation

A surge tank between the conduit and the penstock reduce the water hammer but creates mass oscillation between the reservoir and the surge tank. The mass oscillation is affiliated to opening and closing of the turbine. In case of closing, the water flow from the reservoir to the turbine will flow into the surge tank when the penstock is filled up. The inertia in the system causes the rise of the water level in the surge tank higher than the level in the reservoir. The pressure difference between the reservoir and the surge tank causes the water to start to flow in the opposite direction. This effect is known as mass oscillation [14]. To ensure stability of the mass oscillations in the surge tank, the Thoma criterion is often used. The criterion states that the cross-section of a surge tank needs to be bigger than the Thoma cross-section, in order to be stable. The Thoma cross-section is [15]:

$$A_{th} = 0.016 * \frac{M^2 * {A_P}^{1.5}}{H_n} \tag{3.5}$$

Where

A_{th} Thoma cross-section $[m^2]$

M Mannings value

H_n Nominal water head $[m]$

3.1.3 Waterway time constant

When stability is to be considered, the waterway time constant is important. The waterway time constant is defined as the acceleration time of the water masses from zero to rated water flow between the nearest free surface upstream to the nearest free surface downstream of the turbine [14]:

$$T_w = \frac{Q_n}{g * H_n}\left(\frac{L}{A}\right) \tag{3.6}$$

T_w Water time constant $[s]$

Q_n Nominal flow rate $[m^3/s]$

In order to achieve good stability, the waterway time constant should be less than 1.

3.2 Hydropower unit

It is essential to have a sufficient amount of rotating mass in the system to ensure frequency stability. This chapter explains the functionality of the turbine and generator, the rotating masses and associated requirements.

3.2.1 Turbine and Generator

A Francis turbine is installed in Sundsbarm power plant, and Hjartdøla power plant has a Pelton turbine installed. Francis turbines are used for medium head (30 -700 m) where the guide vane regulates the amount of water flow entering the turbine runner. Pelton turbines are used for high head (300 – 4000 m) and the nozzles regulate the water jet which hit the buckets mounted around the runner [16].

The potential energy of the reservoir is converted into kinetic energy of the water flow in the waterway. The flow is converted in the turbine into mechanical power on the shaft [16]:

$$P_m = \eta \rho g Q H_n \tag{3.7}$$

Where

P_m	Mechanical power $[MW]$
η	Turbine efficiency
ρ	Water density $[kg/m^3]$
g	Acceleration of gravity $[9.81\ m/s^2]$
Q	Flow rate $[m^3/s]$

The turbine shaft is mounted to the shaft of the synchronous generator. The generator converts the mechanical power into electrical power delivered to the grid. The synchronous generator consists of a rotating and a stationary part, named rotor and stator. By applying a DC current to the rotor windings, the rotor transforms into an electromagnet. The turbine runner turns the rotor via the shaft which produces a rotating magnetic field present in the air gap between the rotor and the stator. When the rotor rotates, forces from the magnetic fields produce three-phase voltages in the stator windings. The frequency of the generated voltage in the stator winding and the rotor speed is related by [17, 7]:

$$f = \frac{n \cdot p}{60} \tag{3.8}$$

Where

f	Frequency $[Hz]$
n	Rotational speed $[rev/min]$
p	Number of pole pares

The turbine exerts a mechanical torque τ_m in one direction which causes the shaft to rotate and the generator exerts an electrical torque τ_e in the direction opposite which retards the motion. This makes the unit rotate at angular frequency ω as shown in Figure 3.1.

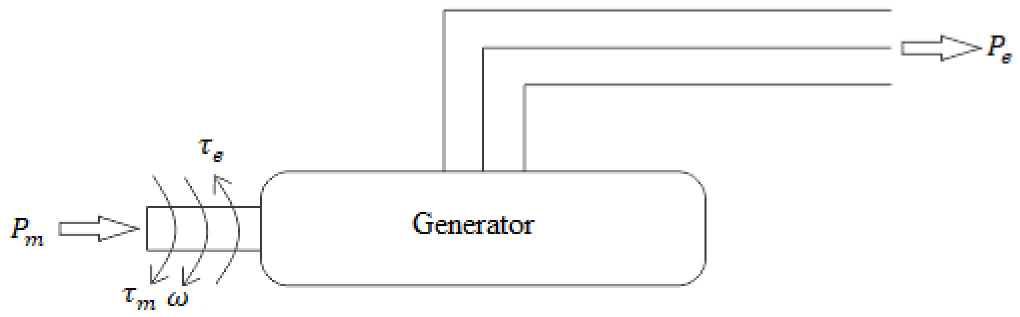

Figure 3.1: Torque balance

The mechanical and electrical torque are expressed as [18]:

$$\tau_m = \frac{P_m}{\omega_m} \tag{3.9}$$

$$\tau_e = \frac{\mathrm{P_e}}{\omega_e} \tag{3.10}$$

Where

τ_m Mechanical torque $[Nm]$

τ_e Electrical torque $[Nm]$

ω_m Mechanical angular frequency $[rad/sec]$

ω_e Electrical angular frequency $[rad/sec]$

P_e Electrical power $[MW]$

In steady-state, the electrical torque is equal to the mechanical torque, taking mechanical losses into account, and the angular frequency remains as constant. The swing equation describes when an imbalance between mechanical and electrical torque occurs. The swing equation is the basis for understanding how inertia affects the frequency changes. The swing equation can be seen in many forms. Here, in p.u [18]:

$$\frac{d\omega}{dt} = \frac{1}{2H}(P_m - P_e) \tag{3.11}$$

Equation (3.9) shows that an imbalance between the mechanical and electrical power of a machine causes frequency derivative. Hence, in a power system with a large number of generators connected to the grid, the rate of change of frequency is dependent on the imbalances and the total amount of inertia in the system [3].

3.2.2 Rotating mass time constant

The rotating masses in the hydropower unit causes inertia in the accelerating time of the rotational speed. This has a positive effect on the control system since the governor has time to make changes before the frequency derivative becomes too large [14]. The rotating masses time constant defines the time it takes to accelerate the turbine and generator from zero to rated angular velocity [14]:

$$T_a = \frac{J * \omega_n^2}{P_n} \tag{3.12}$$

Where

T_a Mechanical time constant $[s]$

ω_n Rated angular velocity $[rad/sec]$

P_n Rated turbine power $[W]$

The time constant is in the range of 5-7 s for larger machines. In order to achieve good stability, the relationship between the rotating masses and the waterway time constant $\frac{T_a}{T_w}$ should be over 4 according to FIKS [19].

The relationship between the rotating mass time constant and the inertia constant can be written as [18]:

$$T_a \approx 2H \tag{3.13}$$

3.3 Governor system

Figure 3.2 shows a block diagram of a simplified governor system of a single-input-single-output (SISO) system.

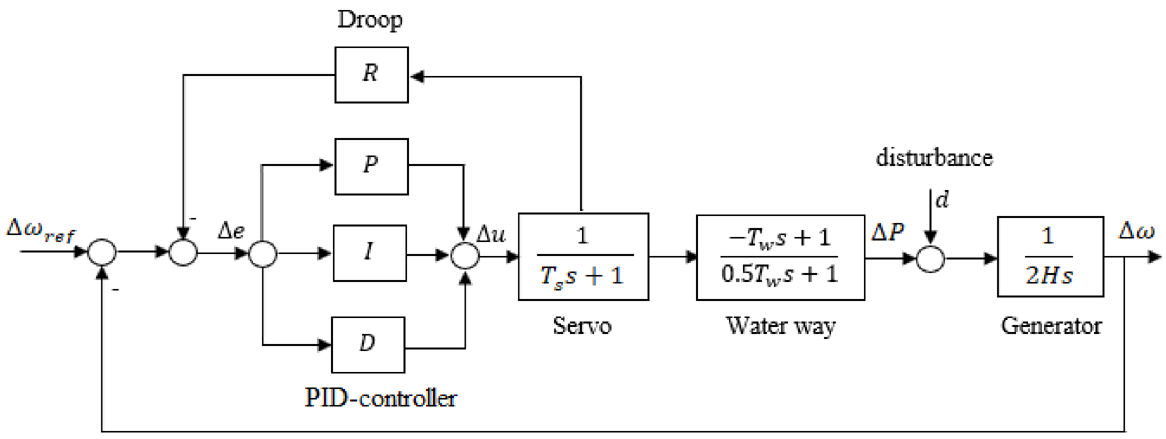

Figure 3.2: Block diagram of simplified governor system

If a disturbance d enters the system the speed of the rotating mass changes, and the system frequency alters. An error Δe occurs between the actual frequency $\Delta\omega$ and the reference frequency $\Delta\omega_{ref}$. Therefore, there is a need for a turbine governor to compensate for the error by changing the valve position. A control signal Δu is performed to the servo in order to change the valve position. The valve position depends both on the droop R and the dynamic (PID) setting of the governor, and the basic governor properties [19]. Therefore, the governor system uses two negative feedback loops. The first one measure the system frequency, as explained above, and the second feedback loop makes sure that the droop is maintained.

3.3.1 PID-controller

According to FIKS, hydropower units $\geq 10\ MVA$, and smaller if possible, shall have a turbine governor installed for active frequency control [19].

Most governors utilized for frequency control today are Proportional–Integral–Derivative (PID) controllers. The PID-controller is given by the formula [20]:

$$\Delta u(t) = \underbrace{K_p \Delta e(t)}_{\text{P-term}} + \underbrace{\frac{K_p}{T_i}\int \Delta e(\tau)d\tau}_{\text{I-term}} + \underbrace{K_p T_d \frac{d\Delta e(t)}{dt}}_{\text{D-term}} \tag{3.14}$$

The proportional gain K_p, the integral time T_i and the derivative time T_d are the PID-controller parameters.

The purpose of the proportional term is to reduce the error by increasing the control signal. The P-term will not achieve zero error in practice and therefore the reference value will not be reached by the P-term alone. The proportional term contributes to a faster control loop, but if the controller gain becomes too large, the control loop becomes unstable [20].

The integral term is the most important term in the controller, because the I-term gives zero steady-state error. The I-term changes the value until the error becomes zero and is relative slowly [20].

The derivative term contributes to a faster control. If the error increase, the derivative time is positive, and the derivative contributes with a positive value to the control variable. This will give a faster control. There is a disadvantage using the D-term, because it may give a very unsteady high frequent control signal due to noise in the process measurement, and such noise is always present. Therefore, the D-term is often set to zero, like a PI-controller [20].

3.3.2 Servo

The servo system is the part of the system that performs the physical actions of the control signal provided by the PID-controller. The servo time constant T_s is based on 100 % valve opening and should be 0.4 s or less [19].

3.3.3 Droop

The grid consists of several generators operating in parallel. For a stable load division between the generators, each governor is provided with a droop characteristic, as shown in Figure 3.3. Otherwise, each governor will try to restore the nominal frequency by changing the power generation. This means that the power generation is distributed more or less randomly over the generator, which is an unwanted situation [12]. Droop setting for generators ≥ 1 MVA should be set from 1 to 12%, according to FIKS [19].

The droop for a generator is expressed as the slope of the curve between power and frequency [12]:

$$R = -\frac{\Delta f / f_n}{\Delta P / P_n} \; [pu] \tag{3.15}$$

Where

Δf Frequency change $[Hz]$

f_n Nominal rated frequency $[Hz]$

ΔP Change in active power $[MW]$

P_n Nominal rated power $[MW]$

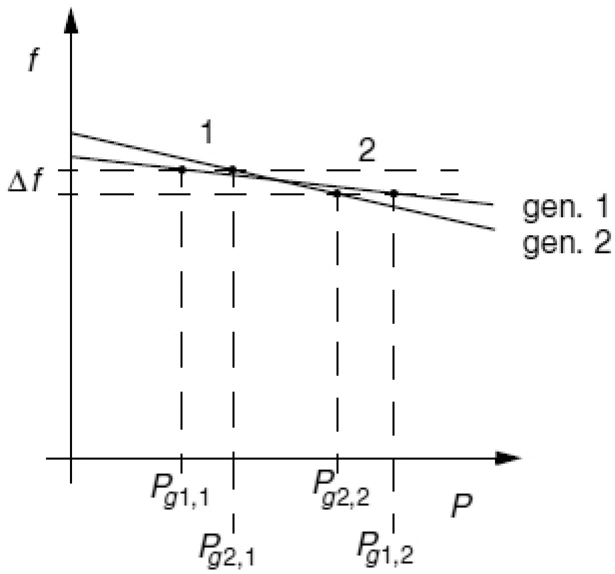

Figure 3.3: Droop characteristics for two generators in parallel [12]

It is the power system frequency characteristic λ that relates the difference between scheduled and actual system frequency to the amount of generation required to correct the power imbalance for a large power system [12]:

$$\lambda = -\frac{\Delta P}{\Delta f}\ [MW/Hz] \tag{3.16}$$

3.3.4 Skogestad's PID tuning method

A simplified description of Skogestad's PID tuning method is given in this subchapter.

Skogestad's method is a model-based tuning method where the governor parameters are expressed as functions of the process model parameters. Skogestad's formulas for a process with integrator and time delay are [20]:

$$K_p = \frac{1}{K_i(T_c + \tau)} \tag{3.17}$$

$$T_i = c(T_c + \tau) \tag{3.18}$$

Where

K_p Proportional gain

K_i Integrator gain $[1/s]$

T_c Time constant of the governor system $[s]$

τ Time delay $[s]$

Skogestad suggests using:

$$T_c = \tau \tag{3.19}$$

$$c = 2 \tag{3.20}$$

The parameter values can be found from a step response experiment for the open loop system without a governor, as shown in Figure 3.4.

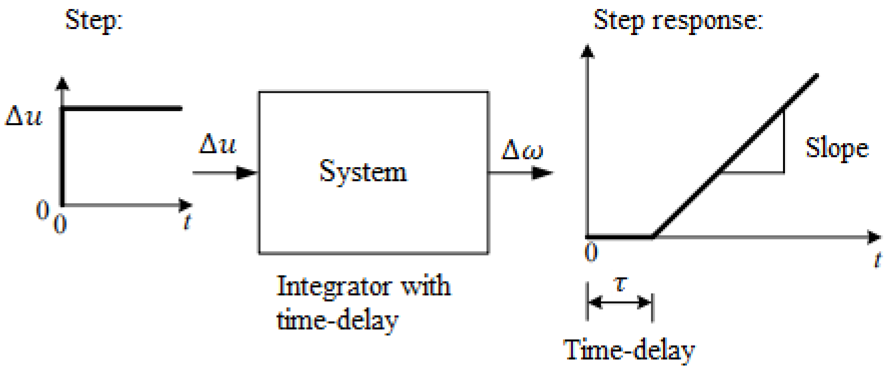

Figure 3.4: Step response [20]

The slope S of the step response can be expressed as:

$$S = K_i \cdot \Delta u \tag{3.21}$$

3.3.5 Stability analysis

According to FIKS, a satisfactory stability for sseperat operation is achieves when the phase margin is in range of 25° to 35° and the gain margin is in the range of 3 dB to 5 dB [19].

The governor system behaviour can be analysed by looking at the frequency response of a system. The frequency response is a frequency dependent function which expresses how a sinusoidal signal of a given frequency on the system is transferred through the system. The frequency response can be presented graphically in for example a Bode diagram or a Nyquist diagram. It is most common to use a Bode diagram to present the gain and phase of a system. The Bode diagram consists of a gain diagram and a phase diagram with logarithmic ω-axis [21].

A system with transfer function $H(s)$ from input to output can be analysed by setting $s = j\omega$ into the transfer function to obtain the complex quantity $H(j\omega)$, which is the frequency response function. The gain is the absolute value of $H(j\omega)$:

$$A(\omega) = |H(j\omega)| \tag{3.22}$$

and the phase is the angle of $H(j\omega)$:

$$\varphi(\omega) = \angle H(j\omega) \tag{3.23}$$

The gain-axis is usually drawn with decibel (dB) as unit. The decibel value of the gain is calculated as:

$$|H(j\omega)|[dB] = 20lg|H(j\omega)| \tag{3.24}$$

Further, the Bode diagram is used to find the gain margin ΔK and the phase margin φ as shown in Figure 3.5. The gain margin is the distance between 0 dB and where the curve crosses the phase crossover frequency, ω_{180}, expressed as [22]:

$$\Delta K = \frac{1}{|H(j\omega_{180})|} \tag{3.25}$$

The phase margin is defined as the distance from the phase to -180° at the amplitude crossover frequency, ω_c, expressed as [22]:

$$\varphi = \angle H(j\omega_c) - (-180°) \tag{3.26}$$

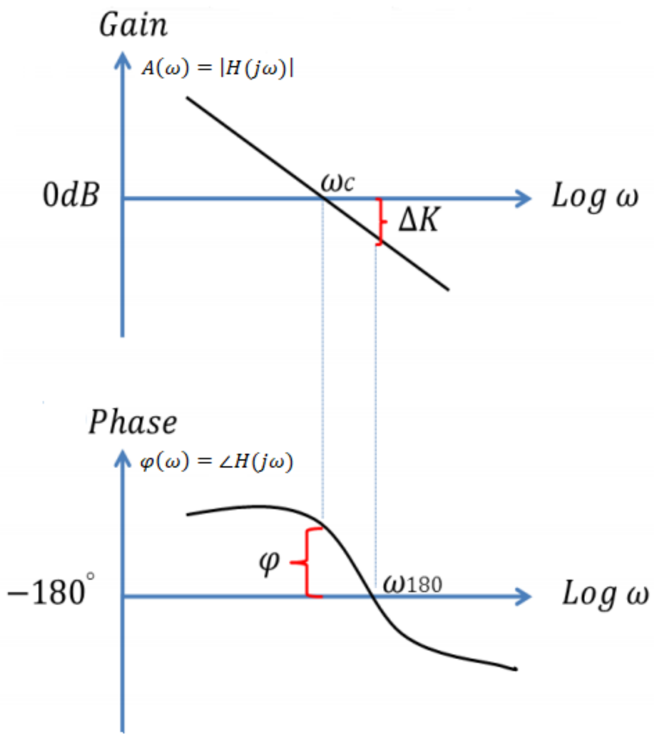

Figure 3.5: Example of Bode Diagram [23]

4 Requirements for FCR-N/D

The aim of developing new technical requirements for FCR is to improve the frequency quality and ensure stability at normal operation in the range of 49.9 - 50.1 Hz and ensure that the system handles dimensional fault at disturbances in the range of 49.9 - 49.5 Hz and 50.1 - 50.5 Hz. The requirements are defined as the dynamic performance, i.e. the ability to damping the amplitude of imbalances, and the robust stability, i.e. stability in the “worst case” Nordic system [24, 25].

4.1 Prequalification

In order for hydropower units to participate in the FCR markets, the units have to be prequalified. The need for a prequalification process is stated in the ENTSO-E System Operation Guideline. The prequalification process includes verification of the properties of the hydropower unit and accomplishment of prequalification tests who shall ensure that all necessary technical requirements are fulfilled [26].

The following tests are included in the prequalification process:

- Step and ramp response tests to determine the capacity and verify the stationary performance requirements.
- Sine tests to verify the dynamic performance requirements and the stability requirements for the FCR units.

During the test, the control signal is replaced by a synthetic signal to determine how the FCR unit responds to frequency deviation [26]. The unit is tested together with the power system which means that the system regulated against is different compared to current FIKS requirements where the unit becomes tested in sperate operation.

4.2 Step and ramp test

In the stationary state, at a nominal frequency of 50.0 Hz shall neither the FCR-N or the FCR-D capacity be activated. However, at frequencies equal to or below 49.9 Hz and equal to or above 50.1 Hz shall 100% of the FCR-N capacity be activated. At frequencies equal or below 49.5 Hz and equal or above 50.5 Hz shall 100 % of the FCR-D upward or downward capacity be activated, respectively. The contribution from each unit shall be designed to be stationary linear with respect to the frequency deviation [26]. The FCR-N capacity is calculated by using the FCR-N step response test in subchapter 4.2.1 and the FCR-D capacity is obtained from the FCR-D step ramp response test described in subchapter 4.2.2.

4.2.1 FCR-N step response test

During the FCR-N step response test, the frequency step input signal applied to the governor is [26]:

- 50.00 Hz → 50.05 → 50.00 → 49.90 → 50.00 → 50.10 → 50.00 Hz.

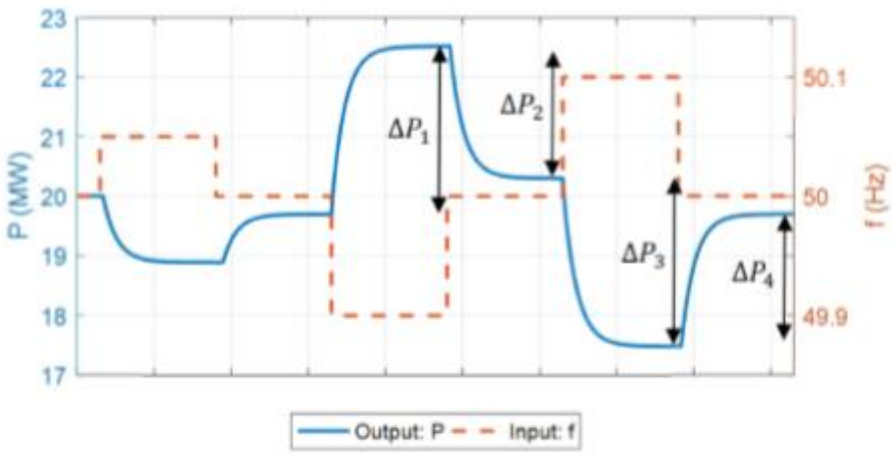

Figure 4.1: FCR-N step response sequence [27]

The step response sequence consists first of a minor step to clear the effect of backlash, then two major steps to determine the capacity. The active power response must be stabilized after each frequency step change before the next frequency step is applied to determine the correct average of the power response [27]:

$$\Delta P = \frac{|\Delta P_1| + |\Delta P_2|}{2} \tag{4.1}$$

Hydropower plants have often a backlash in their control system because the mechanical equipment does not immediately respond to changes in the control system. The total backlash is calculated as [27]:

$$2D = \frac{\big||\Delta P_1| - |\Delta P_2|\big| + \big||\Delta P_3| - |\Delta P_4|\big|}{2} \tag{4.2}$$

Finally, the FCR-N capacity can be calculated as [27]:

$$C_{FCR-N} = \frac{|\Delta P_1| + |\Delta P_3| - 2D}{2} \tag{4.3}$$

4.2.2 FCR-D step and ramp response test

The step response tests for upwards and downwards regulation are performed with the following applied frequency [26]:

- 50.00 Hz → 49.90 → 49.70 → 49.90 → 49.50 → 49.90 Hz, for upwards regulation
- 50.00 Hz → 50.10 → 50.30 → 50.10 → 50.50 → 50.10 Hz, for downwards regulation

From this step response tests, the steady-state FCR-D activation, ΔP_{ss}, is found from 49.9 Hz to 49.5 Hz for FCR-D upwards and from 50.1 Hz to 50.5 Hz for FCR-D downwards.

The frequency ramp applied to the system has a slope of -0.30 Hz/s from 49.9 Hz to 49.0 Hz for upwards regulation and a slope of 0.30 Hz/s from 50.1 Hz to 50.5 Hz for downwards regulation.

As shown in Figure 4.2, the ramp tests are used to find activated power ΔP_{5s} and activated energy $E_{supplied}$ 5 seconds after the start of the ramp. Activated energy is determined by integrating the area under the curve according to [26]:

$$E_{supplied} = \int_{t}^{t+5s} \Delta P(t)dt \tag{4.4}$$

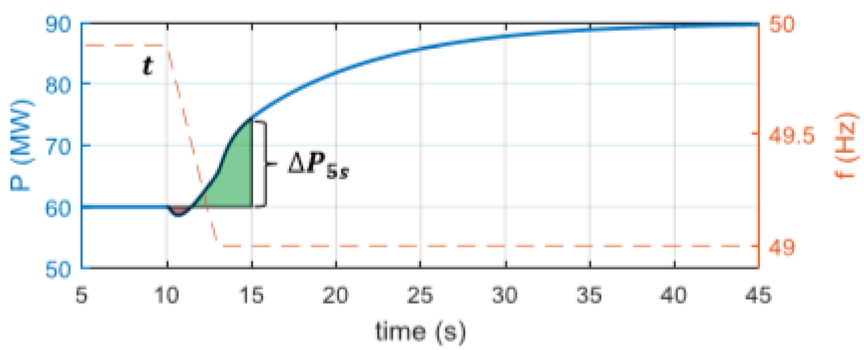

Figure 4.2: Calculation of FCR-D upwards capacity

After these step and ramp tests, the FCR-D capacity is calculated as [26]:

$$C_{FCR-D} = min\left(\frac{\Delta P_{5s}}{0.93}, \Delta P_{ss}, \frac{E_{supplied}}{1.8s}\right) \tag{4.5}$$

4.3 Sine test

In subchapter 3.3.5 it is explained how the frequency response can be found from transfer function. Here, sine tests are used to obtain a set of transfer function values at discrete time periods. The transfer function values are a mathematic representation of the dynamic behaviour of an FCR unit. Each of these transfer functions describes the relationship between the frequency input and the change in power output when the system is subjected to a sinusoidal signal at a different time period. The time periods for the FCR-N and FCR-D tests ranging from 10 - 300 s and 10 - 50 s, respectively [27]. Figure 4.3 illustrates an example of a sine test.

The system is performed with a sinusoidal signal at 50.0 Hz with amplitude A_f of 0.1 Hz:

$$f(t) = f_0 + A_f \sin(\omega t) \tag{4.6}$$

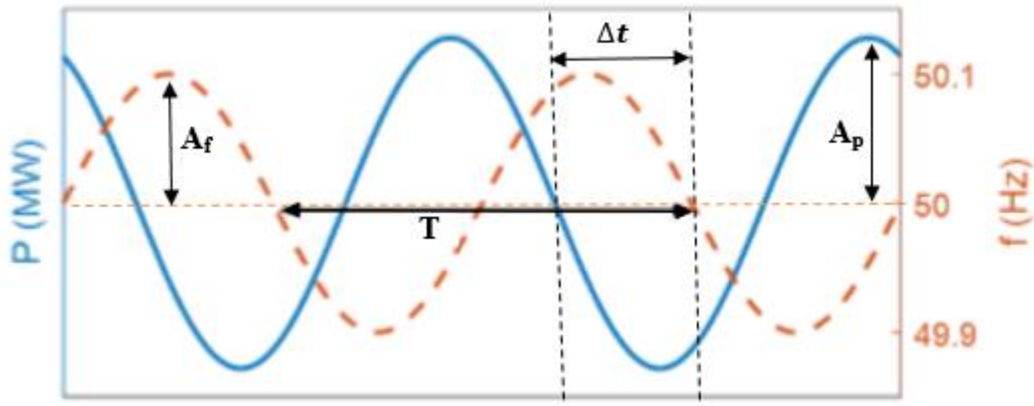

Figure 4.3 Sinusoidal frequency response with corresponding power output [26]

The angular frequency can be calculated according to the time period T as [27]:

$$\omega = \frac{2\pi}{T} \tag{4.7}$$

The transfer function for a certain time period is defined as the magnitude of the output and the phase shift of the power output relative to the input signal, known as gain and phase.

The non-normalized gain of the transfer function can be calculated by divide the amplitude of the power response A_p with the frequency amplitude A_f [27]:

$$|FCR(j\omega)| = \frac{A_p}{A_f} \tag{4.8}$$

The phase φ of the transfer function can be calculated as [27]:

$$\varphi = Arg\big(F(j\omega)\big) = \Delta t \frac{360°}{T} \tag{4.9}$$

Where Δt is the time difference in seconds of the input frequency and the output power response.

To make the transfer function of the gain nondependent of the FCR capacity, the normalization factor, e, is obtained [27]:

$$e = \frac{h * \Delta P}{A_f} \tag{4.10}$$

Where h is the backlash scaling factor based on the total backlash in equation (4.2). The scaling factor can be found in Table 4.1. ΔP is the stationary power change from equation (4.1).

Table 4.1: Backlash scaling factor, h, as a function of total backlash, $2D_{pu}$ [27].

$2D_{pu}$	0.00	0.01	0.02	0.03	0.04	0.05	0.06
h	1	0.999	0.998	0.997	0.996	0.994	0.992
$2D_{pu}$	0.07	0.08	0.09	0.10	0.11	0.12	0.13
h	0.99	0.988	0.986	0.984	0.981	0.979	0.976
$2D_{pu}$	0.14	0.15	0.16	0.17	0.18	0.19	0.20
h	0.974	0.971	0.968	0.965	0.962	0.959	0.956
$2D_{pu}$	0.21	0.22	0.23	0.24	0.25	0.26	0.27
h	0.953	0.95	0.946	0.943	0.94	0.936	0.932
$2D_{pu}$	0.28	0.29	0.30				
h	0.929	0.925	0.921				

Finally, using equation (4.8) and (4.10) the normalized gain can be calculated as [27]:

$$|F(j\omega)| = \frac{|FCR(j\omega)|}{e} \tag{4.11}$$

The normalized gain and phase at different time periods can then be used to draw a Bode diagram to illustrate a visual representation of the response of the FCR unit. Further, the gain and phase can be expressed as FCR-vectors plotted in a complex plane. The gain of the corresponding transfer function value representing the length of the vector and the phase representing the angle between the vector and the real axis. The FCR-vectors have an imaginary axis (y) and a real axis (x) and always start from the origin, point (0,0). The endpoints of the (x, y)-coordinates can be calculated as [27]:

$$x = |F(j\omega)| \cos[Arg(F(j\omega))] \tag{4.12}$$

$$y = |F(j\omega)| \sin[Arg(F(j\omega))] \tag{4.13}$$

The FCR-vectors is defined as the transfer function of the FCR unit $F(s)$ and is further used to verify the dynamic performance requirement and the stability requirement.

4.4 Stability requirement

A method to determine the stability of a system is to trace how a sinusoidal signal propagates in the feedback loop. Stability analysis of a feedback system can be done by plotting the loop gain in a Nyquist diagram. The loop gain is defined as [24]:

$$L(s) = F(s)G(s) \tag{4.14}$$

s	Laplace operator ($s = j\omega$)
$L(s)$	Transfer function of the loop gain
$F(s)$	Transfer function of the FCR unit response
$G(s)$	Transfer function of the power system

The Nyquist curve is obtained from the loop gain plotted in the complex plane at varying angular frequency when the Laplace operator s is replaced by the complex value $j\omega$. The system is required to be stable if the Nyquist curve does not encircle the Nyquist point (-1,0j) and the does not enter the stability margin circle with a radius of 0.411 p.u. stated in the report "FCR-N design of requirement" [25]. An example of a Nyquist diagram is shown in Figure 4.4.

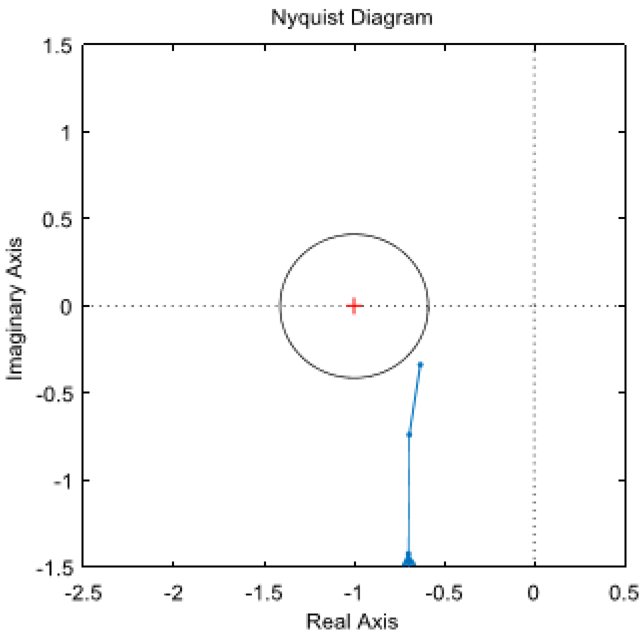

Figure 4.4: FCR-N/D stability requirement (black) and an example response (blue) [26]

4.4.1 Verification of FCR-N stability requirement

The FCR-N stability requirement is verified using a Nyquist diagram, as described above. The Nyquist curve is obtained from the loop gain transfer function in equation (4.14) for the different angular frequencies corresponding to time periods of 10-50 s [27].

$$L_{FCR-N}(s) = F(s)G_{FCR-N}(s) \tag{4.15}$$

Where

$L_{FCR-N}(s)$	Loop gain transfer function for FCR-N delivery
$F(s)$	Transfer function of the FCR response
$G_{FCR-N}(s)$	Power system transfer function for FCR-N

The power system transfer function consists of the term $-\frac{600MW}{0.1\,Hz}$ which is the required power system frequency characteristic for FCR-N.

$$G_{FCR-N}(s) = -\frac{600MW}{0.1Hz}\cdot\frac{f_0}{S_{n-min}}\cdot\frac{1}{2H_{min}s + K_{f-min}\cdot f_0} \tag{4.16}$$

Where

S_{n-min}	System loading of the low inertia system $[MW]$
H_{min}	Inertia constant of the low inertia system $[s]$
K_{f-min}	Load frequency dependence of the low inertia system

The stability is tested for “worst case” Nordic system, thus the parameters for the power system is for the low inertia system. This implies an uncertainty for the low inertia system, given by the radius of the stability margin circle, is allowed before instability. Thus, there is an uncertainty margin which can either be in the plant or in the FCR - unit response [24].

4.4.2 Verification of FCR-D stability requirement

The stability requirement for FCR-D is verified in the same as the FCR-N stability requirements and the FCR-vectors is in the same way as for FCR-N if the unit using the same controller parameters. However, the power system transfer function is different [27].

$$G_{FCR-D}(s) = -\frac{\Delta P_{ss}}{C_{FCR-D}}\cdot\frac{1450MW}{0.4Hz}\cdot\frac{f_0}{S_{n-min}}\cdot\frac{1}{2H_{min}s + K_{f-min}\cdot f_0} \tag{4.17}$$

The power system transfer function is multiplied by two terms. The term $\frac{\Delta P_{ss}}{C_{FCR-D}}$ which represents the scaling of capacity and the term $-\frac{1450MW}{0.4\ Hz}$ which is the required power system frequency characteristic for FCR-D. The scaling of capacity is needed to ensure stability for the actual frequency characteristic of the system, as unit FCR capacity can be lower than the steady-state power (will lead to higher system regulating strength).

The stability of the unit is then evaluated in a Nyquist diagram.

4.5 Dynamic performance requirement

The dynamic performance requirement is a mainly specifying that the amplitude of an imbalance is to be reduced to a certain size. The performance requirements are evaluated for the average inertia system. The transfer function from a disturbance entering the system is defined as [24]:

$$D(s) = \frac{G(s)}{1 + L(s)} \tag{4.18}$$

Where

$D(s)$ Disturbance transfer function

4.5.1 Verification of FCR-N dynamic performance requirement

The dynamic performance requirement for FCR-N delivery is defined as a diagram with a pre-qualified requirement curve and a curve representing the unit response together with a representation of the power system. In order to fulfil the FCR-N dynamic performance requirement shall the response curve lay below the requirement curve, as shown in Figure 4.5.

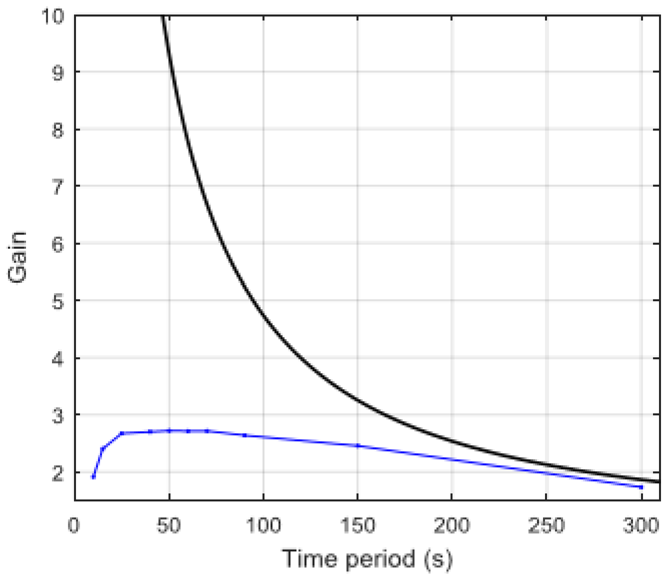

Figure 4.5: FCR-N dynamic performance requirement (black) together with an example response (blue) [26]

The requirement curve is defined as the absolute value of the inverse of the transfer function of the expected system active power disturbance profile, scaled by a factor of 1.05 in order to account for measurement uncertainty [27]:

$$\left|\frac{1}{\frac{1}{70s+1}}\right| * 1.05 \tag{4.19}$$

The response curve is obtained from the absolute value of the disturbance transfer function in equation (4.18) [24]:

$$\left|\frac{G_{FCR-N}(s)}{1+F(s)G_{FCR-N}(s)}\right| \tag{4.20}$$

The power system transfer function for FCR-D at normal performance is [27]:

$$G_{FCR-N}(s) = -\frac{600MW}{0.1Hz} \cdot \frac{f_0}{S_{n-avg}} \cdot \frac{1}{2H_{avg}s + K_{f-avg} * f_0} \tag{4.21}$$

Where

S_{n-avg} System loading of the average inertia system $[MW]$

H_{avg} Inertia constant of the average inertia system $[s]$

K_{f-avg} Load frequency dependence of the average inertia system

4.5.2 Verification of FCR-D dynamic performance requirement

The FCR-D dynamic performance is described by the FCR-D capacity by equation (3.5) [27]. There is no specific requirement. However, the hydropower unit should contribute with what it is capable of within 5s. If the unit does not deliver steady-state activation in 5 seconds, its capacity will be scaled. Today's requirement is 50% activation within 5 s and 100% activation within 30 s.

5 Simulation Model

To build up a hydropower model for Sundsbarm and Hjartdøla power plant to perform the tests described in chapter 3, the program Dymola is used. Dymola is a commercial modeling and simulation tools where model components are connected in the same way as a real system. The program is based on the open Modelica modeling language and support libraries of truly reusable components. The library used in this thesis is the Hydro Power Library [29].

The total system is divided into several subsystems, namely reservoir, conduit, surge tank, pressure shaft, downstream, turbine, turbine governor, generator, and grid. Overview of the base model used is shown in Figure 5.1.

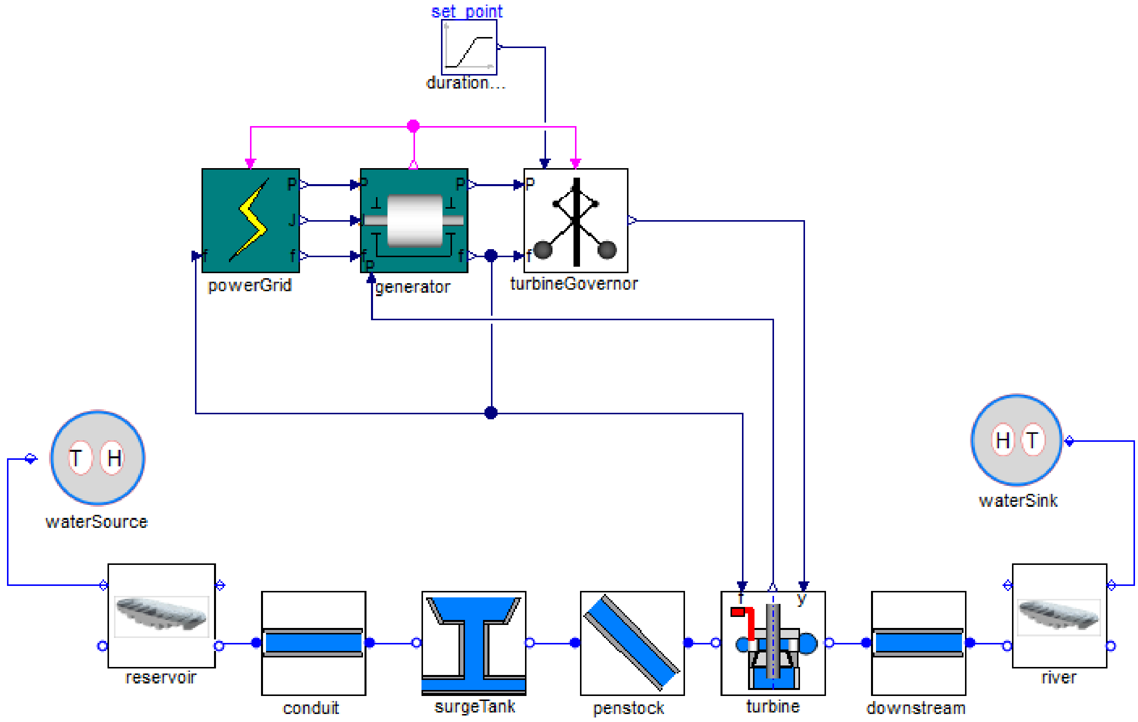

Figure 5.1: Simulation model

The generator is connected to a grid with a big load stabilizing the system and supplementary active power control like aFRR is disabled so the setpoint remains unchanged. During the tests, the frequency input signal to the governor is replaced by a synthetic signal as explained in Chapter 4 .

5.1 Sundsbarm Power Plant

Sundsbarm hydropower plant is located in Seljord municipal in Telemark and is owned by Skagerak Kraft AS. The power plant has been in operation since 1970 and has an average annual production of 439 GWh [29].

5.1.1 Waterway

Sundsbarm power plan utilizes the head of the upper reservoir, Sundsbarmvatn, and the lower reservoir, Seljordsvatn. Sundsbarmvatn is approximately 12.5 km long and 0.7 km wide and is regulated at an elevation of 574 to 612 meters of sea level. The water flows through a channel to the surge tank and further through the penstock that narrow down to the power station. The draft tube ends in Vallaråi which flows into the lower reservoir, Seljordsvatn. To model the waterway correctly, length, pipe diameter and the elevation of the left and right end of the pipe are derived from technical drawings. The parameters are listed in table Where

A	Cross-section area $[m^2]$

d	Pipe diameter $[m]$

Table 5.1.

Neither the cross-section area or the pipe diameter for the surge tank is specified in the technical drawings. Hence, the Thoma criterion explained in subchapter 3.1.2 with a security factor of +25% is used as the cross-section area of the surge tank. The Thoma cross section is calculated from equation (3.5). Further, the pipe diameters are calculated based on the cross-section area using the equation:

$$A = \frac{1}{4}\pi d^2 \tag{5.1}$$

Where

A	Cross-section area $[m^2]$

d	Pipe diameter $[m]$

Table 5.1: Waterway parameters for Sundsbarm power plant

	Length $[m]$	Pipe diameter $[m]$	Elevation of left end $[m]$	Elevation of right end $[m]$
Channel	6600	5.8	564	541.5
Surge tank	150	3.6	-	-
Penstock	724	3.0	541.5	112.5

5.1.2 Turbine, generator and turbine governor

Sundsbarm power plant has one Francis turbine installed. Data of the turbine and generator found from technical documents are listed in Table 5.2. Turbine flow and efficiency based on the guide vane opening is set directly into the model found from the efficiency curve in Appendix B.

Table 5.2: Parameters of the hydropower unit in Sundsbarm power plant

Rated power of turbine $[MW]$	103
Rated flow rate of the turbine $[m^3/s]$	24
Rated head of the turbine $[m]$	480
Rated rotational speed $[rev/min]$	500
Inertia of the generator $[kg \cdot m^2]$	212 500
Number of generator poles	12

According to FIKS, the servo time constant should be 0.4 or less. Hence, the servo time constant is set to 0.2s and the upper and lower limits for the servo motor velocity is given from Skagerak Kraft As and is set to ± 0.12 1/s.

Sundsbarm power plant has a safety valve at the turbine. This shall ensure that the pressure in the system does not exceed the permissible level by dropping water past the turbine by rapid closing of the guide vane. Hence, the closing time T_L for the guide vane is approximately 7 s, whine the closing time for the safety valve is approximately 25 s. The valve is not included in the model.

In the simulation model, the turbine governor model is of standard PID structure with three gains K_p, K_i and K_d. The gains correspond to K_p, $\frac{K_p}{T_i}$ and $K_p \cdot T_d$ of the classical configuration of equation (3.14). As mentioned earlier, the D-term is often not used and is not included in the simulation model. The PI parameters in the turbine governor are tried tuned by Skogestad's method and the parameters obtained are tested in the simulation model. This is explained and discussed in chapter 6.

5.2 Hjartdøla Power plant

Hjartdøla hydropower plant is located in Hjartdal municipal in Telemark and is owned by Skagerak Kraft AS. The power plant was put into operation in 1958 and rehabilitated in 2005. There are two Pelton turbines installed with total power of 120 MW and an average annual production of 489 GWh [30].

5.2.1 Waterway

Hjartdøla power plant utilizes the head between the upper reservoir, Breidvatn, and the lower reservoir, Hjartsjåvatnet. Along the channel from the upper reservoir, Breidvatn, to the surge tank there are two side intakes, Vatnartjern (774 m.a.s.l) and Damtjernbekken (760 m.a.s.l). Breidvatn is regulated at elevation of 723 to 749 m.a.s.l. Waterway parameter are derived from technical drawings listed in Table 5.3.

Channel 1 is from Breidvatn to the side intakes, Vatnartjern, channel 2 is from the side intakes, Vatnartjern, to the side intakes, Damtjernbekken, channel 3 is from the second side intakes to the surge tank and channel 4 is from the surge tank to the penstock.

Table 5.3: Waterway parameters for Hjartdøla power plant

	Length $[m]$	Pipe diameter $[m]$	Elevation of left end $[m]$	Elevation of right end $[m]$
Channel 1	2100	4.6	715.5	705
Vatnartjern	-	2-2.5	-	-
Channel 2	1830	4.6	705	700
Damtjernbekken	-	2-2.5	-	-
Channel 3	2200	4.6	700	704
Surge tank	150	3.3	-	-
Channel 4	20	4.6	704	690
Penstock	900	2.6	690	160

5.2.2 Turbine, generator and turbine governor

Hjartdøla power plant has two Pelton turbines installed, but the model consists only of a single turbine to be tested. As with the waterway, the parameters of the turbine and generator is found from technical documents handed out of Skagerak Kraft As. Turbine efficiency based on water flow and valve opening is attached in Appendix B.

Table 5.4: Turbine and generator parameters for Hjartdøla power plant

Rated power of turbine $[MW]$	66
Rated flow rate of the turbine $[m^3/s]$	13.4

Rated head of the turbine $[m]$	555
Rated rotational speed $[rev/min]$	428
Inertia of the generator $[kg.m^2]$	266 000
Number of generator poles	14

The time constant is set to 0.2s as for Sundsbarm power plant. The upper and lower limits for the servo motor velocity is ± 0.12 1/s given by Skagerak Kraft As.

In the same manner as for Sundsbarn power plant, the turbine governor model used is a standard PID, where the D-term is excluded. The PI parameters is obtained and discussed in chapter 6.

6 Tuning and Testing of Turbine Governor

The turbine governors in Sundsbarn and Hjardøla power plants are tried tuned by Skogestad's methode to obtain the PI-parameters. The parameters are used to perform a separate operation detection of stability according to FIKS. The stability analysis is performed by using the simplified block diagram of the governor system, shown in Figure 6.1. The block diagram is similar to the simulation model, except for the waterway that is far more complicated in the simulation model. The block diagram only shows inelastic water and pipes in the penstock and no description of the waterway against the penstock.

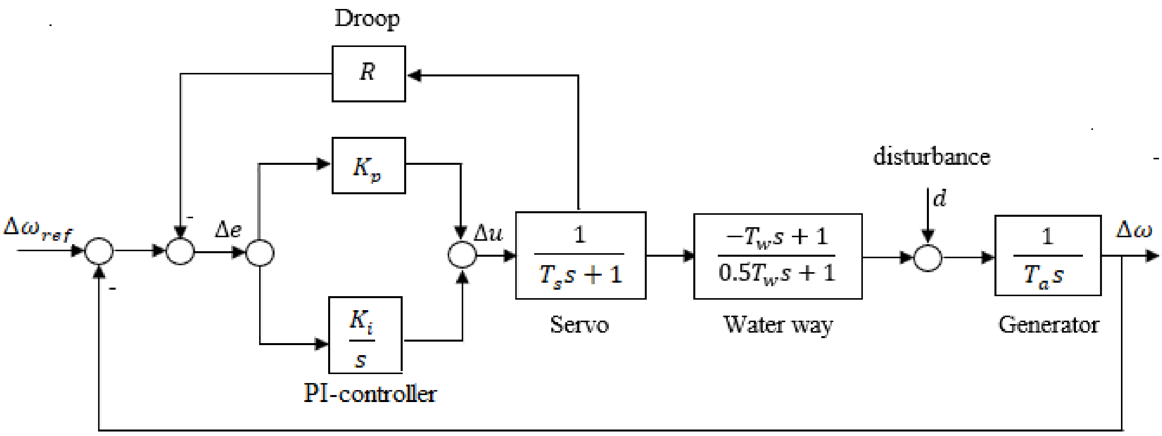

Figure 6.1: Block diagram of simplified governor system

6.1 Skogestad's tuning method

A step response test is performed to the system, shows in Figure 6.1, from $\Delta\omega$ to Δu without feedback in order to obtain the PI-parameters. A step in the control signal Δu is applied to the system. The step respose test are performed in Excel using the transfer functions in the block diagram above. By setting $s = j\omega$, the frequency response can be plotted.

6.1.1 Sundsbarm Power Plant

The parameters used for the step response test for Sundsbarm power plant are listed in Table 6.1.

Table 6.1: System parametes for Sundsbarm power plant

Control signal Δu [%]	10
Servo time constant T_s [s]	0.2

Waterway time constant T_w $[s]$	0.55
Rotational masses time constant T_a $[s]$	5.66

The servo time constant is stated in chapter 5, and the waterway time constant and time rotating masses constant is calculated by equation (3.6) and (3.12).

The frequency response after a step in the control signal Δu is shown in Figure 6.2.

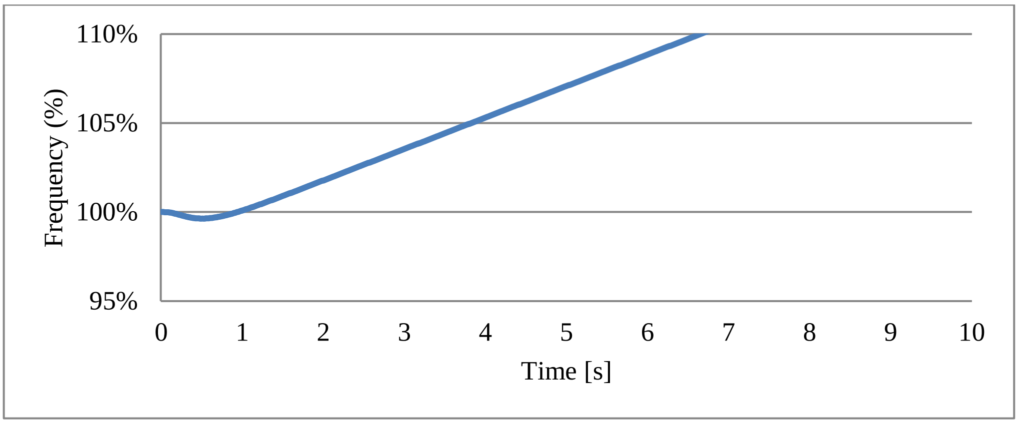

Figure 6.2: The frequency response for Sundsbarm power plant after a step in the control signal Δu

From the step response in Figure 6.2, the time-delay τ and the slope S are determined:

$$\tau = 1.0\ s \tag{6.1}$$

$$S = 1.7\ \frac{\%}{s} \tag{6.2}$$

Using equation (3.21), the integrator gain K_i is calculated:

$$K_i = 0.17 \frac{1}{s} \tag{6.3}$$

The proportional gain K_p and the integrating time T_i are found from equation (3.17) and (3.18)

$$K_p = 2.9 \tag{6.4}$$

$$T_i = 4.0\ s \tag{6.5}$$

According to FIKS about classification of governor dynamics, gives $K_p > 3$ and $T_i < 4$ good properties.

6.1.2 Hjartdøla Power Plant

The parameters used for the step response test for Hjartdøla power plant are listed in table 6.2.

Table 6.2: System parameters for Hjardøla power plant

Control signal Δu [%]	10
Servo time constant T_s $[s]$	0.2
Waterway time constant T_w $[s]$	0.42
Rotational masses time constant T_a $[s]$	8.09

In the same manner as for Sundbarm power plant, the servo time constant is stated in chapter 5, and the waterway constant and rotating masses constant is calculated by equation (3.6) and (3.12).

The frequency response for Hjartdøla power plant is shown in Figure 6.2

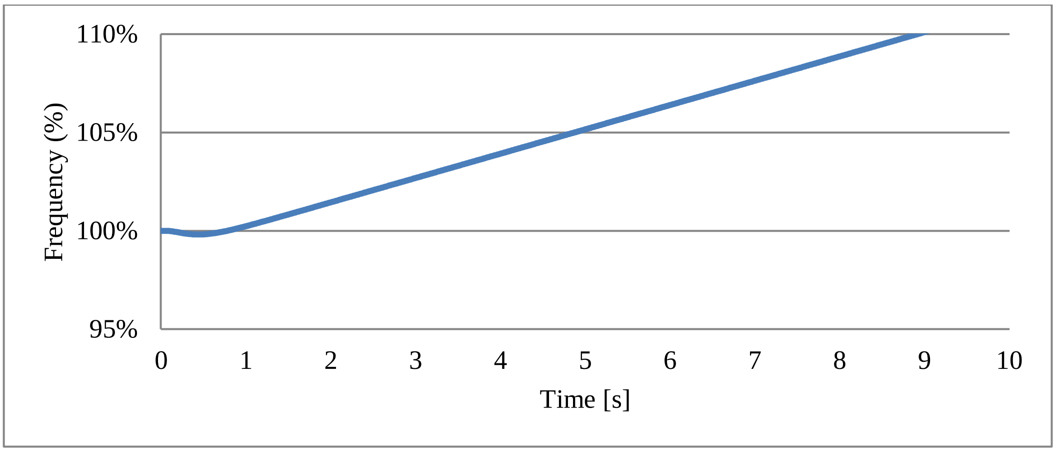

Figure 6.3: The frequency response for Sundsbarm power plant after a step in the control signal Δu

The time-delay τ and the slope S are found from the step response in Figure 6.3

$$\tau = 0.9\ s \tag{6.6}$$

$$S = 1.2\ \frac{\%}{s} \tag{6.7}$$

this gives

$$K_i = 0.12\frac{1}{s} \tag{6.8}$$

Then, the gain K_p and the integrating time T_i can be found by equation (3.17) and (3.18)

$$K_p = 4.6 \tag{6.9}$$

$$T_i = 3.6\ s \tag{6.10}$$

6.2 Stability analysis according to FIKS

This subchapter shows stability analysis in separate operations to check whether the controller tuned by Skogestad's method satisfies the requirements for phase and gain margins within the range of 25 ° to 35 ° and 3 dB to 5 dB, respectively.

The analysis are performed to the system with governor tuned by Skogestads methode. The system without feedbacks is plotted in Excel using the transfer functions from the block diagram in Figure 6.1. By setting $s = j\omega$, the frequency response can be plotted.

6.2.1 Sundsbarm Power Plant

The governor parameters obtained from Skogestad's method used in stability analysis for Sundsbarm power plant is listed in Table 6.2.

Table 6.2: PI-parameters from Skogestad's methode for Sundsbarm power plant

Parameter	**Values**
$K_p[pu]$	2.9
$K_i\ [pu]$	0.73

The phase and gain at angular frequencies from -0.1 to 0.1 rad/s are calculated using equation (3.23) and (3.24), respectively. The gain and phase are used to construct a Bode diagram to find the gain and phase margin, as shown in Figure 6.4.

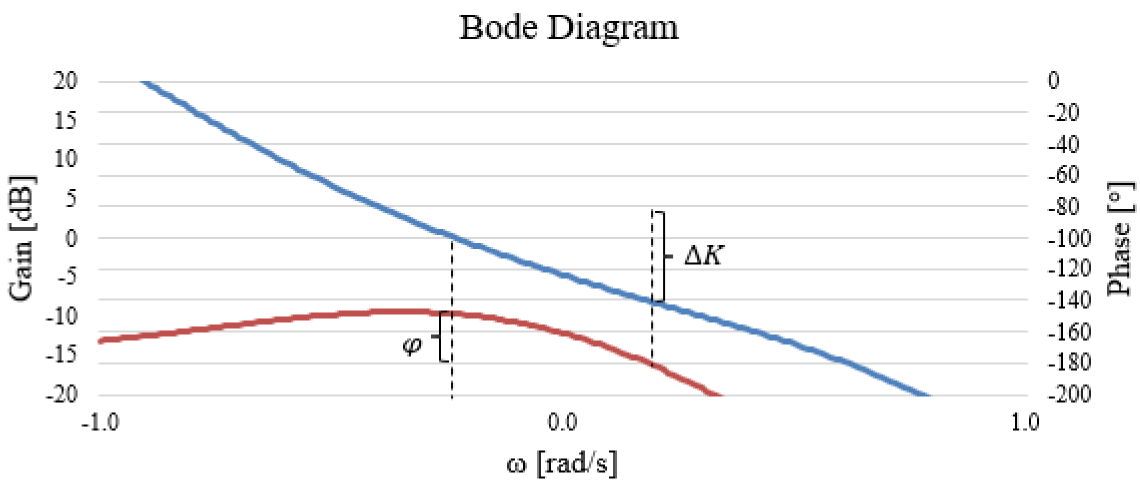

Figure 6.4: Bode diagram for Sudsbarm. The red curve is the gain and the blue curve is the gain.

The gain margin ΔK and phase margin φ can be found from the Bode diagram in using equation (3.25) and (3.26):

$$\Delta K = 8.5\ dB \tag{6.11}$$

$$\varphi = 32° \tag{6.12}$$

The gain margin appears to be too high in relation to the stability requirements in separate operation. Therefore, it is advisable to increase the proportional gain K_p. By setting $K_p = 5$, the phase and gain margin give satisfied stability according to FIKS.

6.2.2 Hjartdøla Power Plant

The PI-parameters obtained from Skogestad's method used in stability analysis for Hjartdøla power plant is stated in Table 6.3.

Table 6.3: PI parametes for Hjartdøla power plant

Parameter	**Values**
Proportional gain $K_p[pu]$	4.6
Integrator gain K_i $[pu]$	1.28

The phase and the gain are calculated using equation (3.23) and (3.24), respectively. The gain and phase are used to construct a Bode diagram to find the gain and phase margin, as shown in Figure 6.5.

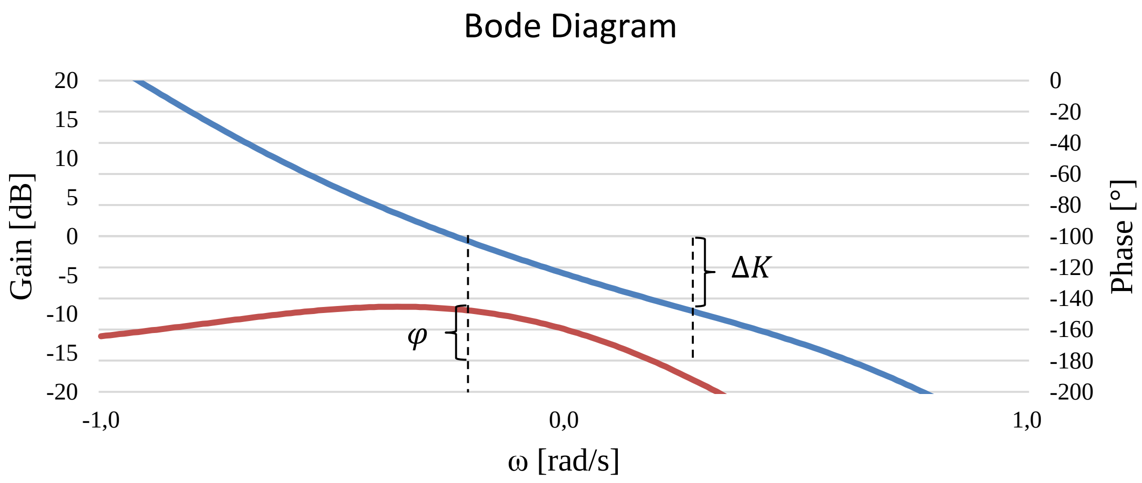

Figure 6.5: Bode diagram for Hjardøla. The red curve is the gain and the blue curve is the gain.

The gain and phase margin are found from Figure 6.5 using equation (3.25) and (3.26):

$$\Delta K = 9.5\ dB \tag{6.13}$$

$$\varphi = 36° \tag{6.14}$$

The gain margin ΔK and the phase margin φ appears to be too high in according to the stability requirements. Therefore, it is advisable to increase both the proportional gain K_p and the integrator gain K_i in order to verify the stability requirement in separate operation.

6.3 Testing of the turbine governors

Skagerak Kraft As has handed out a set of commissioning reports of the turbine governors in Sundsbarm and Hjardøla power plants. The commissioning reports are attached in Appendix C for Sundsbarm power plant and Appendix D for Hjartdøla power plant. These are the basis for deciding whether the behaviour of the turbine governors in the simulation models reflects the real governors in Sundsbarm and Hjartdøla power plants.

The simulation models for Sundsbarm and Hjartdøla power plants are first tested around the parameters obtained from Skogestad’s tuning method. The simulations shows a marginally stable system for both power plants hence the output signal does not return to near a common steady-state. This is not desired and does not match the commissioning reports which shows asymptotic stable systems, where the input signal drives the output to steady-state.

Figure 6.6 shows a marginally stable system for Sundsbarm power plant.

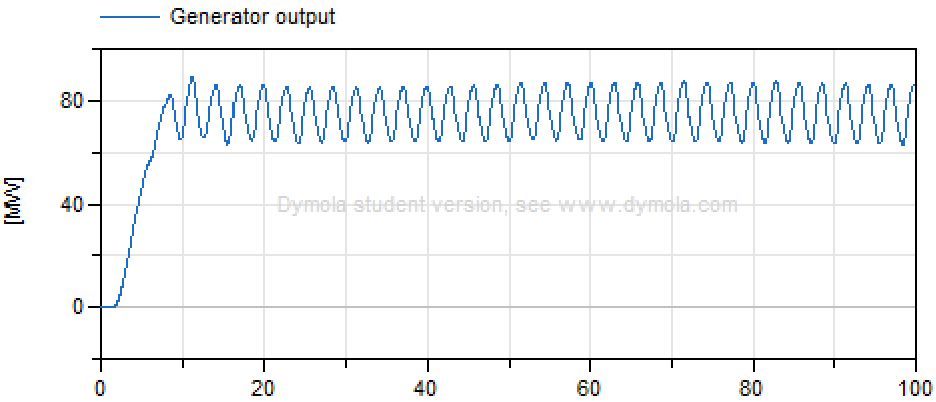

Figure 6.6: Power response for Sundsbarm power plant tuned by Skogestad's method

It is therefore attempted to reduce the PI-controller parameter to achieve asymptotic stability response for the plants. It is tested for different parameters and best succeeds with the parameters $K_p = 0.3$ and $K_i = 0.2$ for Sundsbarm power plant and $K_p = 0.2$ and $K_i = 0.1$ for Hjartdøla power plant. Hence, the gain is considerably decreased to get the same behaviour of the simulation models as the commissioning reports. Figure 6.7 shows the power response in Sundsbarm power plant after reducing the PI-parameters.

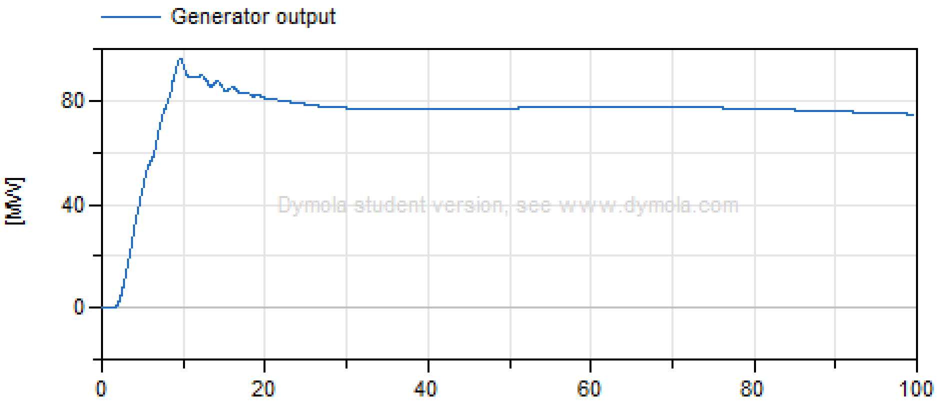

Figure 6.7: Power response for Sundsbarm power plant complete tuned.

Further, the behaviour of pressure in front of the turbines when closing the turbines at different set points is compared with the reports.

In the commissioning reports for Sundsbarm, the pressure oscillates fast over a shorter time period due the elasticity in the water and pipe when closing the turbine, before the pressure is stabilized as longer oscillations. In the simulation model the pressure is higher compared to the commissioning reports due to the safety valve that is not included in the model. Equation (3.4) shows that faster closing time of the valve gives greater pressure rise. Hence, the pressure is higher in the simulation model.

In the commissioning reports for Hjardøla, the pressure oscillates fast over a longer time when closing the turbine. This is also the case in the simulation model due to the elasticity effect.

The time period of the pressure surges is also approximately equal in the simulations and the reports. Based on the comparisons with the reports, the simulation models are considered, together with the supervisor, to be sufficient representations of Sundsbarm and Hjartdøla power plant.

7 Prequalification tests

The prequalification tests are performed on the simulation model for Sundsbarm power plant and the model for Hjartdøla power plant. The simulation parameters for the power system is are stated in [27].

Table 7.1: Power system paramerers for average and low inertia system

Parameters	**Average inertia system**	**Low inertia system**
Nominal grid frequency f_0 $[Hz]$	50	50.0
System loading $S_n [MW]$	42 000	23 000
Inertia constant $H[s]$	4.5	5.2
Load frequency dependence K_f	0.01	0.005

7.1 Sundsbarm Power Plant

The tests are performed for Sundsbarm power plant at both maximum load with maximum droop and minimum load with minimum droop. The simulation parameters for Sundsbarm power plant are listed in Table 7.2.

Table 7.2: Simulation parameters for Sundsbarm power plant

Proportional gain K_p $[pu]$	0.3
Integrator gain K_i $[pu]$	0.2
Maximum turbine load P_{max} $[MW]$	100
Minimum turbine load P_{min} $[MW]$	60
Maximum droop $R_{max}[\%]$	12
Minimum droop $R_{min}[\%]$	4

Only the results from the maximum load with maximum droop are presented in the report. Results from minimum load with minimum droop is attached in Appendix E and is shortly discussed in chapter 8.

7.1.1 FCR-N step response

The FCR-N step response test is used to find the capacity of the FCR-N unit. The step response sequence is applied to the system 10 minutes after start of the simulation, so the generator is stabilized around the set point. The duration of each frequency step change is set to 5 minutes, so the power response is stabilized before the next frequency change is applied.

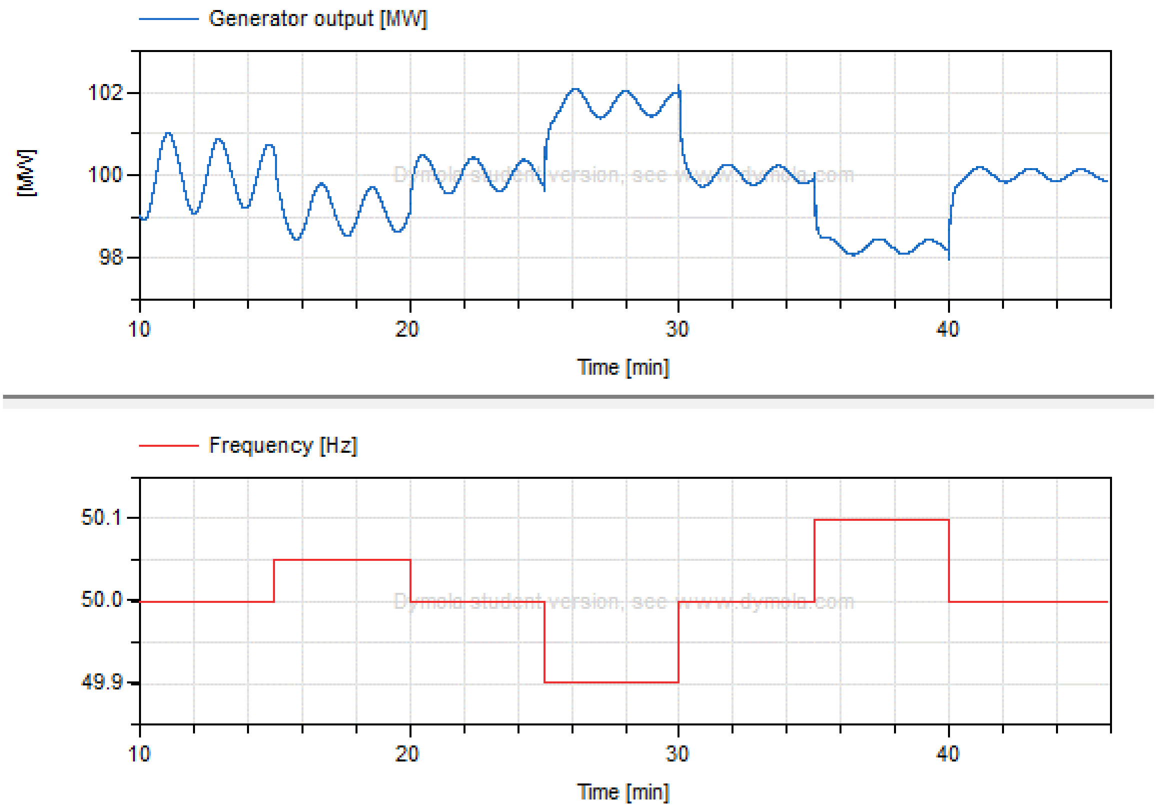

Figure 7.1: FCR-N step response maximal load at Sundsbarm

The change in active power response is found by using the mean value of each stabilized power step response:

Table 7.3: FCR-N step response Sundsbarm Power Plant

Frequency $[Hz]$	Step	ΔP $[MW]$
49.9	ΔP_1	1.72
50.0	ΔP_2	1.72
50.1	ΔP_3	1.73
50.0	ΔP_4	1.73

The average of the active power step response can then be calculated from equation (4.1)

$$\Delta P = \frac{1.72 + 1.73}{2} = 1.73\ MW \tag{7.1}$$

There is approximate no backlash in the system, as shown in Figure 7.1, and the backlash factor is therefore set to $h = 1$, as stated in table 1. Further, the factor is neglected for all calculations since the backlash in the simulated systems are almost zero and the factor constitutes minimal differences in the results. Therefore, the FCR-N capacity, given by equation (4.3), is set to be equal to the average active power:

$$C_{FCR-N} = \frac{1.72 + 1.73}{2} = 1.73\ MW \tag{7.2}$$

From the power response, the normalization factor e is calculated using equation (4.10):

$$e = \frac{1.73}{0.1} = 17.3MW/Hz \tag{7.3}$$

7.1.2 Sine test

In the sine tests, a sinusoidal signal with amplitude A_f of 0.1 is applied to the system for 10 different time periods between 10-300s, as shown in Table 7.4.

Table 7.4: Parameters from the sine tests at Sundsbarm power plant

$T\ [s]$	$\omega\ [rad/s]$	$\Delta t\ [s]$	$A_p[MW]$	$Gain\ [MW/Hz]$	$Norm\ Gain\ [p.u.]$	$Phase\ [°]$
10	0.6283	3.3	0.63	6.3	0.36	118.8
15	0.4189	5.1	0.80	8.0	0.46	122.4
25	0.2513	9.4	1.03	10.3	0.60	135.4
40	0.1571	16.6	1.28	12.8	0.74	149.0
50	0.1257	21.2	1.37	13.7	0.79	152.6
60	0.1047	25.8	1.39	13.9	0.80	154.8
70	0.0898	30.9	1.41	14.1	0.82	158.9

90	0.0698	40.8	1.60	16.0	0.92	163.2
150	0.0419	66.8	1.76	17.6	1.02	160.3
300	0.0209	151.7	1.78	17.8	1.03	182.0

The angular frequency ω for the certain time periods is calculated by equation (4.7) and plotted in the simulation model to get the correct frequency of the sine wave. From each sine tests, the time difference Δt between the applied frequency and the generator power output is found, as well the amplitude of the power response A_p. Then, the gain and the normalization gain are determined by equation (4.8) and (4.11), respectively. Finally, the phase for each response is obtained from equation (4.9).

To test the dynamic performance and stability of the FCR-N unit, the normalization gain and phase for each response are transformed to vectors in the complex plane by equation (4.12) and (4.13).

Table 7.5: FCR-vectors Sundsbarm power plant

T [s]	Real part (x)	Imaginary part (y)
10	-0.17	0.32
15	-0.25	0.39
25	-0.43	0.42
40	-0.63	0.38
50	-0.70	0.36
60	-0.72	0.34
70	-0.77	0.30
90	-0.88	0.27
150	-0.96	0.34
300	-1.03	-0.04

To test the FCR-N stability, the final stability verification using Nyquist diagram is performed. To obtain the Nyquist curve, the FCR unit transfer function $F(s)$ is multiplied the grid transfer function $G_{FCR-N}(s)$ from equation (4.14):

$$F(s) \cdot \left[-\frac{600MW}{0.1Hz} \frac{f_0}{S_{n-min}} \frac{1}{2H_{min}\, s + K_{f-min} \cdot f_0} \right] \tag{7.4}$$

By setting $s = j\omega$, the Nyquist curve is plotted for angular frequencies corresponding to the time period 10-50 s.

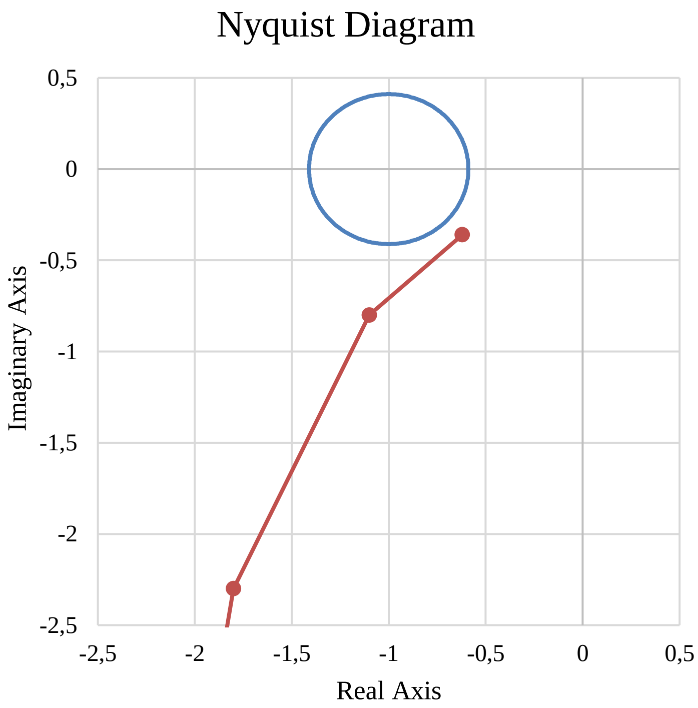

Figure 7.2: FCR-N stability requirement (blue) and the response at Sundsbarn plant (red)

In order to guarantee stable system operation, the Nyquist curve has to pass the stability circle at the right-hand side. Hence, the hydropower unit at maximum load in Sundsbarm is considered stable for FCR-N delivery.

To verify the FCR-N dynamic performance requirement, the response curve (red) is plotted in a diagram together with the FCR-N dynamic performance requirement curve (black), as shown in Figure 7.3. The response curve is obtained by equation (4.20) transformed to complex quantity by setting $s = j\omega$ and plotted for the time period 10-300 s with corresponding angular frequency

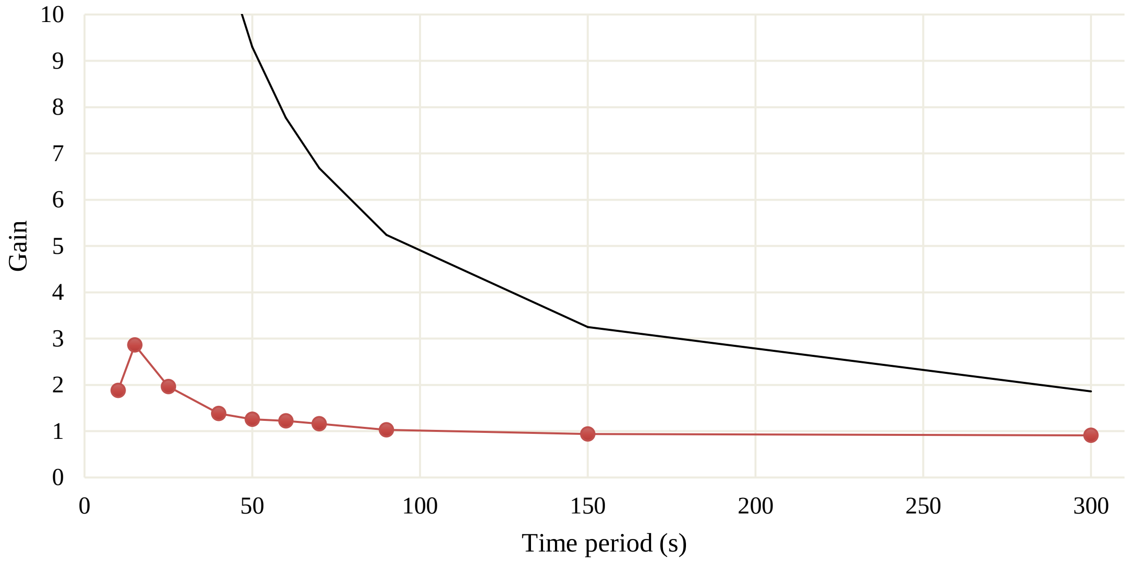

Figure 7.3: FCR-N dynamic performace requirement (black) and the response (red)

The response curve is always below the requirement curve which means that the dynamic performance requirement is fulfilled.

7.1.3 FCR-D upwards regulation

For frequency disturbances at 49.9 Hz and lower, the FCR-D for upwards regulation has to be activated. During the test, the FCR-D unit has not any saturation limit on the controller measurement inputs.

In order to verify the FCR-D dynamic performance, the power response of an input frequency step sequence is simulated.

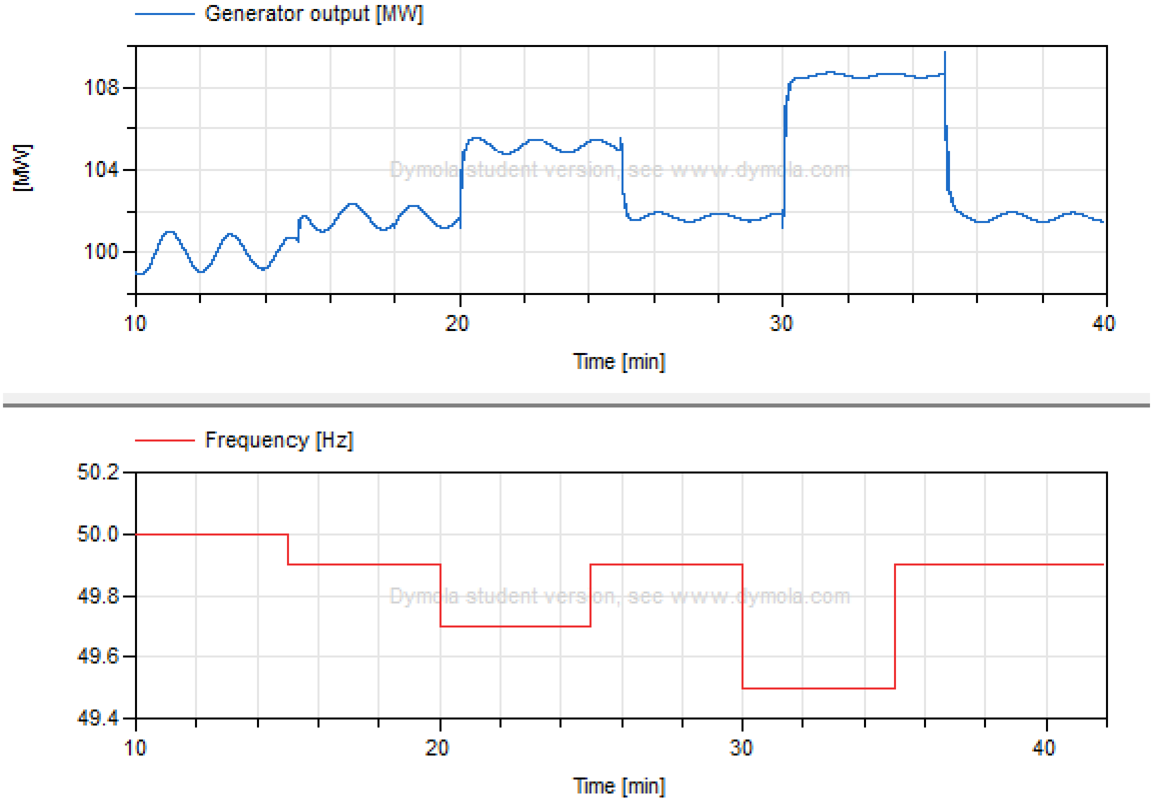

Figure 7.4: FCR-D upwards regulation step response at Sundsbarm power plant

The absolute value of the power response changes in Figure 7.4 are listed in Table 7.6 for each frequency step.

Table 7.6: FCR-D upward regulation step response

Frequency step $[Hz]$	ΔP $[MW]$
50.0 - 49.9	1.7
49.9 - 49.7	3.5
47.7 - 49.9	3.5
49.9 - 49.5	7.1
49.5 - 49.9	7.1

From table 7.6, the steady-state FCR-D activation for upwards regulation is found from the frequency step 49.9-49.5 Hz:

$$\Delta P_{ss} = 7.1MW \tag{7.5}$$

The ramp respons test is performed with a frequency input signal from 49.9 to 49.0 Hz with a slope of $-0.3\ Hz/s$.

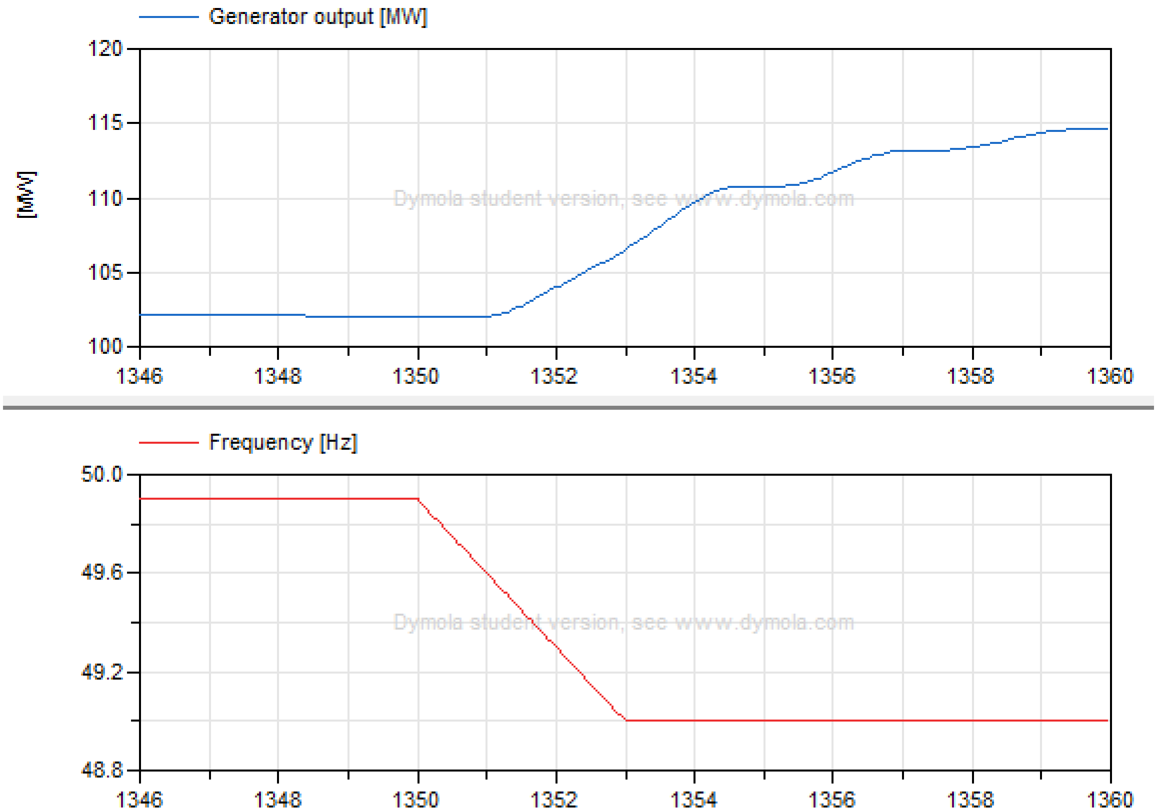

Figure 7.5: Ramp response for upwards regulation at Sundsbarm power plant

The ramp response in Figure 7.5 is used to find the activated power 5 seconds after the start of the ramp:

$$\Delta P_{5s} = 8.7MW \tag{7.6}$$

By calculating the area under the power response curve from the start of the ramp to 5 seconds after the start, the activated energy is calculated:

$$E_{supplied} = 18.3MWs \tag{7.7}$$

Then, the FCR-D capacity is calculated using equation (4.5):

$$C_{FCR-D} = \min(9.4, 7.1, 10.2) = 7.1MW \quad (7.8)$$

As seen in equation (7.8), the results from both the scaling factors $\frac{\Delta P_{5s}}{0.93}$ and $\frac{E_{supplied}}{1.8s}$ are greater than the steady-state activation ΔP_{ss}. This indicates that the governor responds fast enough to activate steady-state power within five seconds.

In order to verify the stability requirements, the FCR-D unit need to fulfil the same requirements as the FCR-N unit. The Nyquist curve is obtained by the FCR unit transfer function $F(s)$ times the scaled grid transfer function $G(s)_{FCR-D}$:

$$F(s) \cdot \left[-\frac{\Delta P_{ss}}{C_{FCR-D}} \frac{1450MW}{0.4Hz} \frac{f_0}{S_{n-avg}} \frac{1}{2H_{avg}s + K_{f-avg} \cdot f_0} \right] \quad (7.9)$$

By setting $s = j\omega$, the Nyquist curve is plotted for different angular frequencies corresponding to the time period 10-50 s.

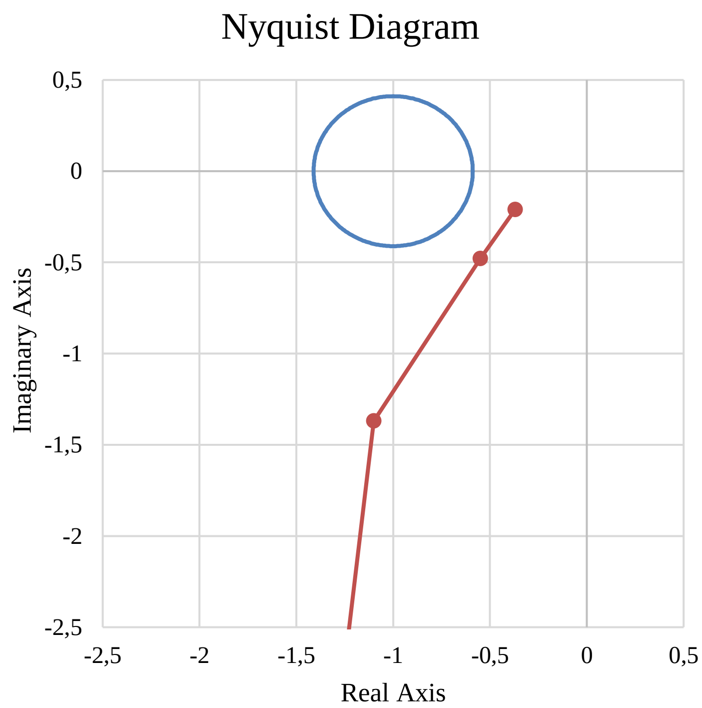

Figure 7.6: Nyquist Diagram for FCR-D downwards regulation at Sundsbarm power plant

The scaling factor of capacity $\frac{\Delta P_{ss}}{C_{FCR-D}}$ is equal to 1, which means that the unit has sufficient capacity compared to its full steady-state activation. Hence, the scaling factor make it easier to fulfil the stability requirements. As shown in figure 7.6, the FCR-D unit qualifies for stability since the Nyquist curve pass the stability margin circle at the right-hand side.

7.1.4 FCR-D downwards regulation

If disturbances lead to frequency at 50.1 Hz and higher, the FCR-D downward regulation shall be activated. In order to test the performance of the FCR-D unit, a frequency step from 50.1 to 50.5 Hz and a ramp from 50.1 to 51.0 Hz with a slope of -0.3 Hz/s is applied to the turbine governor.

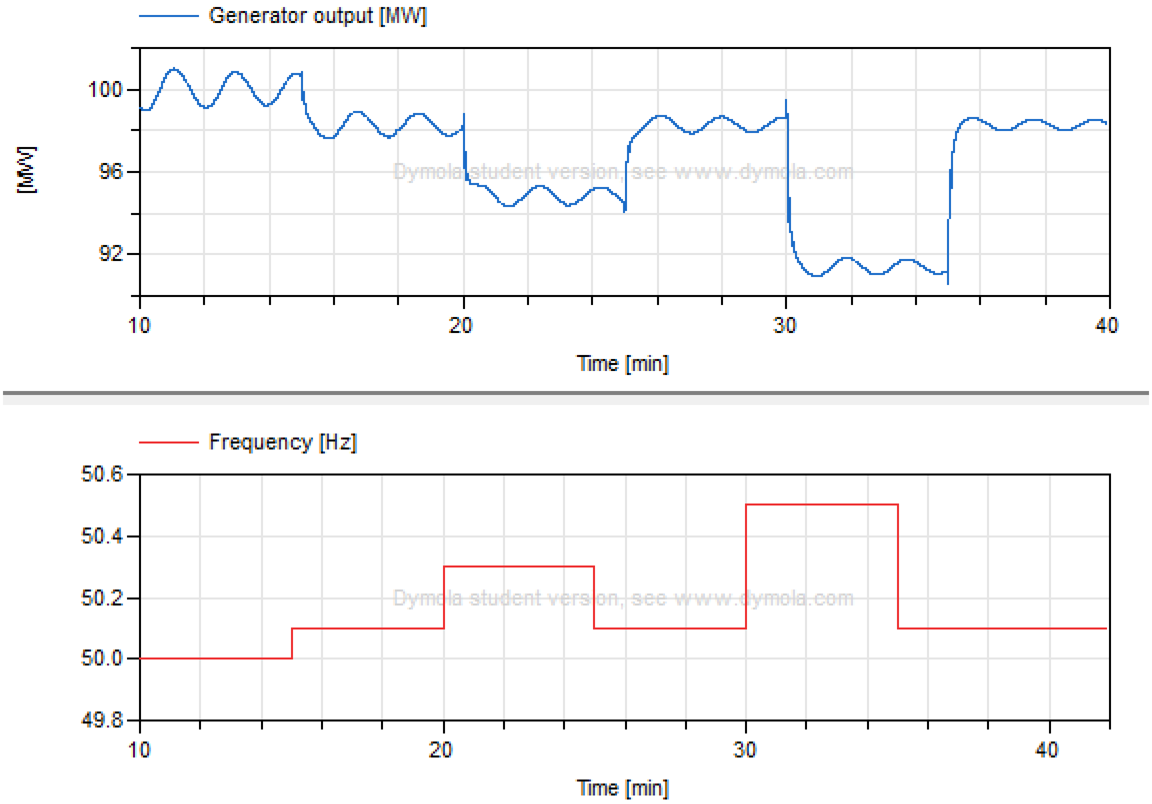

Figure 7.7: FCR-D downwards regulation step response at Sundsbarm power plant

The changes in power response to the applied frequency step are listed in the table 10. The FCR-D unit activate the power linearly in the frequency range from 50.1 Hz to 50.5 Hz thus satisfies the stationary activation requirement.

Table 7.7: FCR-D downwards regulation step response

Frequency step $[Hz]$	ΔP $[MW]$
50.0 - 50.1	1.8
50.1 - 50.3	3.6

50.3 - 50.1	3.6
50.1 - 50.5	7.2
50.5 - 50.1	7.2

From table 7.7, the steady-state activation for FCR-D downwards regulation is obtained from the frequency step 50.1-50.5 Hz:

$$\Delta P_{ss} = 7.2MW \tag{7.10}$$

Figure 7.8 shows the ramp response test of FCR-D downward regulation.

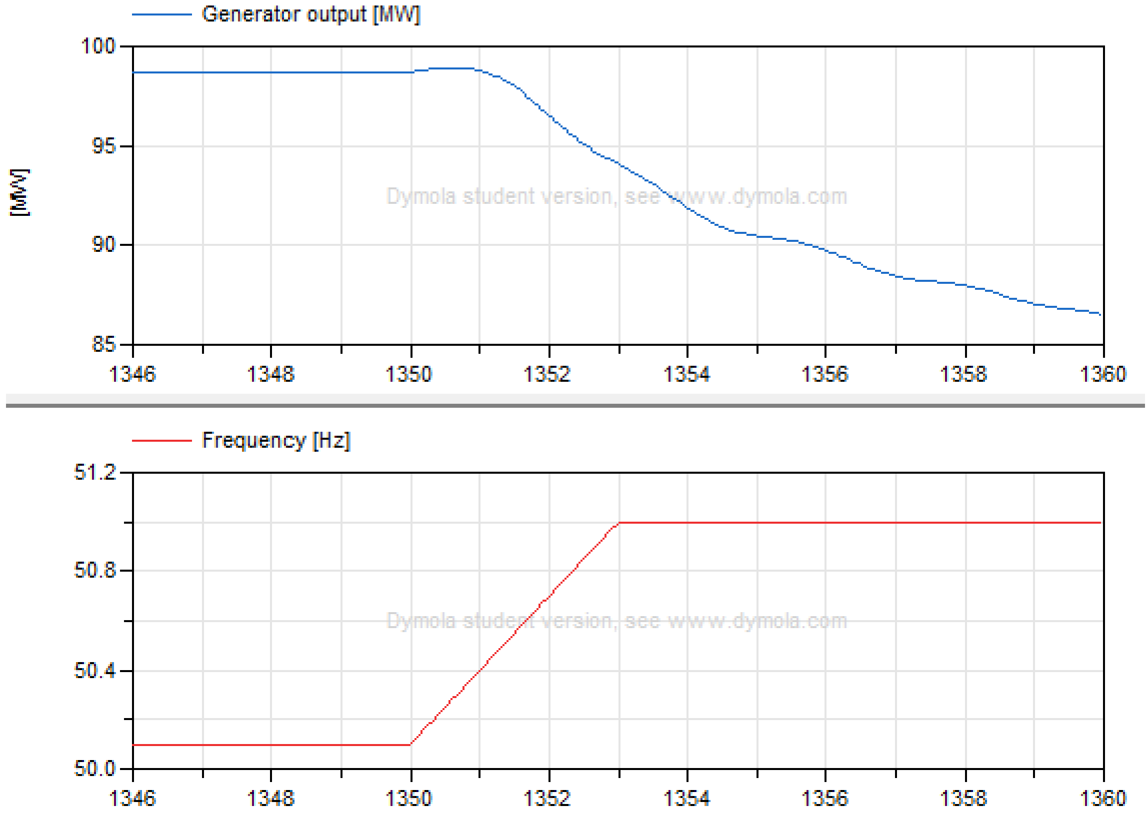

Figure 7.8: FCR-D downward regulation ramp response

The activated power and energy 5 seconds after the start of the ramp can be found from figure 7.8:

$$\Delta P_{5s} = 8.2MW \tag{7.11}$$

$$E_{supplied} = 23.1MWs \tag{7.12}$$

From equation (4.5), the FCR-D downward capacity is calculated:

$$C_{FCR-D_{down}} = \min(8.8, 7.2, 12.8) = 7.2MW \tag{7.13}$$

As for the upwards regulation, the governor responds fast enough to activate steady-state power within five seconds. This indicate a good FCR-D dynamic performance of the unit.

The stability is tested in the same way as for the FCR-D upwards regulation.

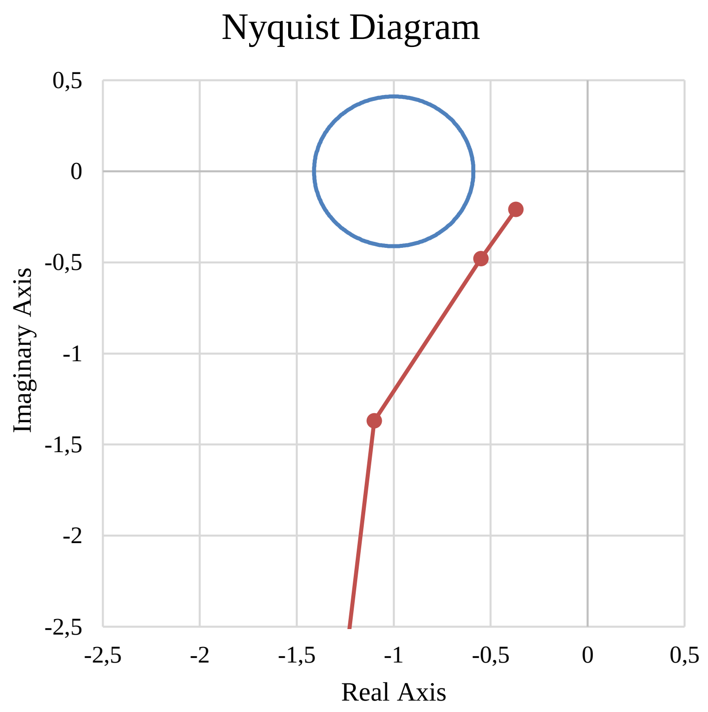

Figure 7.9: Nyquist Diagram for FCR-D downwards regulation at Sundsbarm power plant

Since the scaling factor $\frac{\Delta P_{ss}}{C_{FCR-D}}$ is equal to 1 also for the FCR-D downwards regulation, the Nyquist curve for the upwards and downwards regulation are equally. Hence, the stability requirement for FCR-D downward regulation is fulfilled.

7.2 Hjartdøla Power Plant

The tests to verify the dynamic performance and stability requirements is performed for Hjartdøla power plant at maximum load with minimum droop and minimum load with maximum droop. The simulation parameters for the power plant is listed in Table 7.7

Table 7.8: Simulation parametes for Hjartdøla power plant

Proportional gain K_p $[pu]$	0.2
Integrator gain K_i $[pu]$	0.1
Maximum turbine load P_{max} $[MW]$	60
Minimum turbine load $P_{min}[MW]$	20
Maximum droop R_{max}[%]	12
Manimum droop R_{min}[%]	4

Only the results from the maximum load with minimum droop are presented in the report. Results from minimum load with maximum droop is attached in Appendix D and is shortly discussed in chapter 8.

7.2.1 FCR-N step response

The step response is simulated to determine the FCR-N capacity for Hjardøla power plant. As in the same manner as for the simulations of Sundsbarm power plant, the frequency changes are applied to the system 10 minutes after the start of the simulations. The active power response is stabilized after each frequency step change before the next frequency step change is applied to the system.

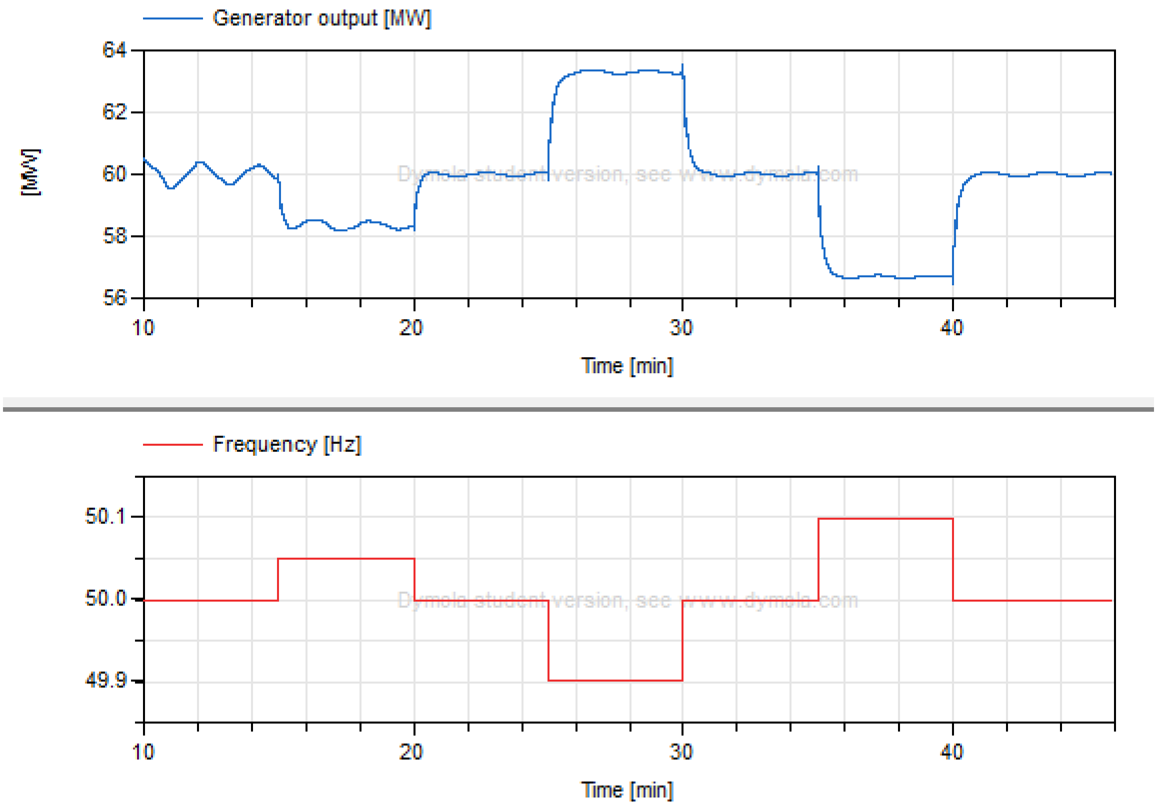

Figure 7.10: FCR-N step response at Hjartdøla power plant

Table 7.9 FCR-N step response Hjartdøla power plant

Frequency $[Hz]$	Step	$\Delta P\ [MW]$
49.9	ΔP_1	3.30
50.0	ΔP_2	3.30
50.1	ΔP_3	3.30
50.0	ΔP_4	3.30

As shown in Figure 7.10, there is no backlash in the system, so the FCR-N capacity is set equal to the active power response:

$$C_{FCR-N} = \frac{3.30 + 3.30}{2} = 3.30\ MW \tag{7.14}$$

The normalization factor is:

$$e = \frac{3.3}{0.1} = 33.0MW/Hz \tag{7.15}$$

7.2.2 Sine tests

A sinusoidal signal is applied to the governor for time periods ranging from 10-300. The values from the sine tests is found in the same manner as for Sundsbarm power plant.

Table 7.10: Vaules from the sine tests for Hjartdøla power plant

T $[s]$	ω $[rad/s]$	$A_p[MW]$	Δt $[s]$	$Gain$ $[MW/Hz]$	$Norm\ Gain$ $[p.u.]$	$Phase$ [°]
10	0.6283	0.76	3.5	7.6	0.23	126.0
15	0.4189	0.89	5.3	8.9	0.27	127.2
25	0.2513	1.21	8.9	12.1	0.37	128.2
40	0.1571	1.68	14.7	16.8	0.51	132.3
50	0.1257	1.94	18.6	19.4	0.59	133.9
60	0.1047	2.14	22.7	21.4	0.65	136.2
70	0.0898	2.30	27.6	23.0	0.70	141.9
90	0.0698	2.53	36.9	25.3	0.77	147.6
150	0.0419	3.14	63.9	31.4	0.95	153.4
300	0.0209	3.26	143.3	32.6	0.99	171.9

By translating the normalization gain and phase obtained in Table 7.10 to FCR-vectors in the complex plane, the dynamic performance and stability can be tested.

Table 7.11: FCR-vector for Hjartdøla power plant

T $[s]$	Real part (x)	Imaginary part (y)
10	-0.14	0.19
15	-0.16	0.22
25	-0.23	0.29

40	-0.34	0.38
50	-0.41	0.43
60	-0.50	0.45
70	-0.55	0.43
90	-0.65	0.41
150	-0.85	0.43
300	-0.98	0.14

The stability is tested by plotting the Nyquist curve in a Nyquist diagram together with stability margin circle. To obtain the Nyquist curve, the FCR transfer function $F(s)$ times the grid transfer function $G_{FCR-N}(s)$ is plotted for angular frequencies corresponding to the time periods from 10 s to 25 s.

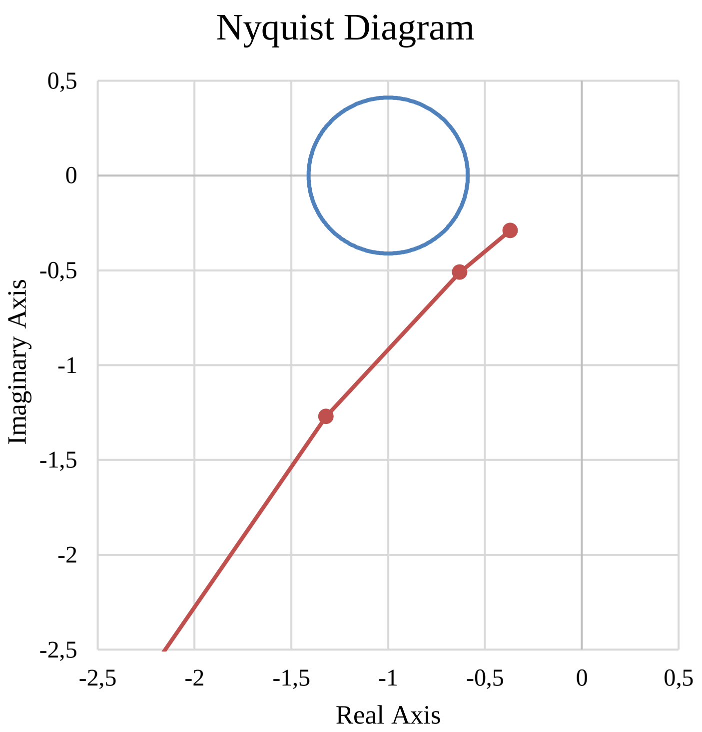

Figure 7.11: Nyquist Diagram for FCR-N at Hjartdøla power plant

The Nyquist curve enter the stability circle on the right-hand side. Hence, the hydropower unit fulfil the stability requirement for FCR-N delivery.

The FCR-N dynamic performance is tested by plotting a curve defined by the FCR-vectors together with a representation of the power system $G_{FCR-N}(s)$ in the same diagram as the pre-defined performance requirement curve.

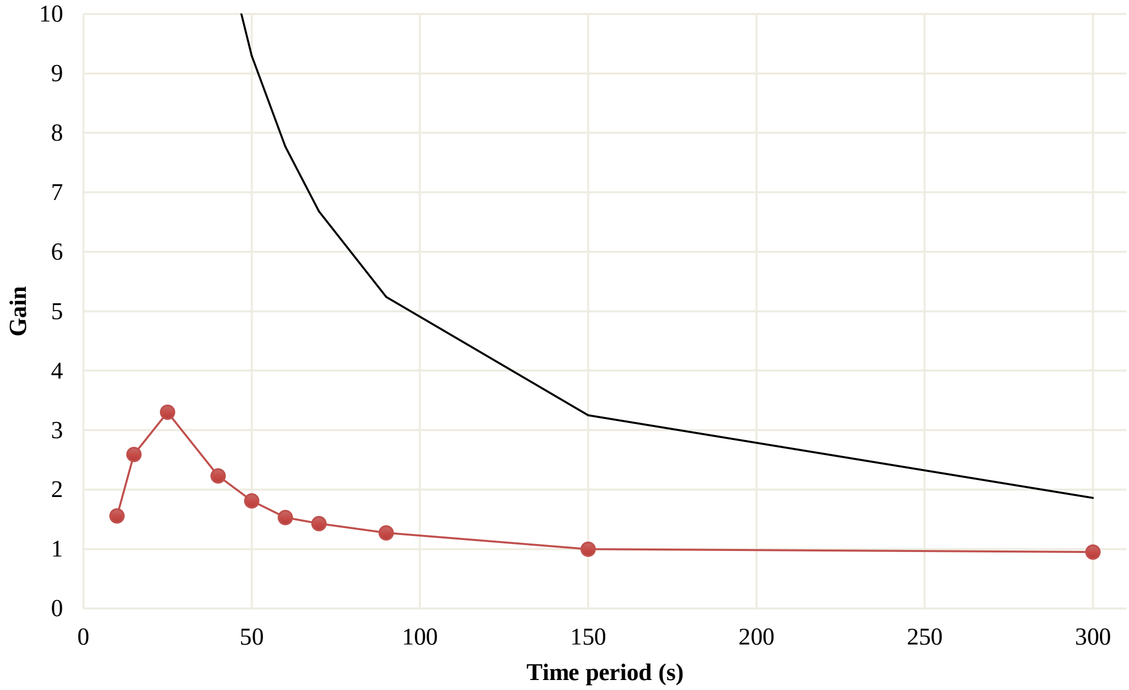

Figure 7.12: Dynamic performance for FCR-N at Hjartdøla power plant

The response curve is below the requirement curve, which state a good dynamic performance of the FCR-N unit.

7.2.3 FCR-D upwards regulation

The FCR-D capacity for upwards regulation is determined by simulating a step response test and a ramp response test. First, the power response to a step response sequence is simulated against the frequency input.

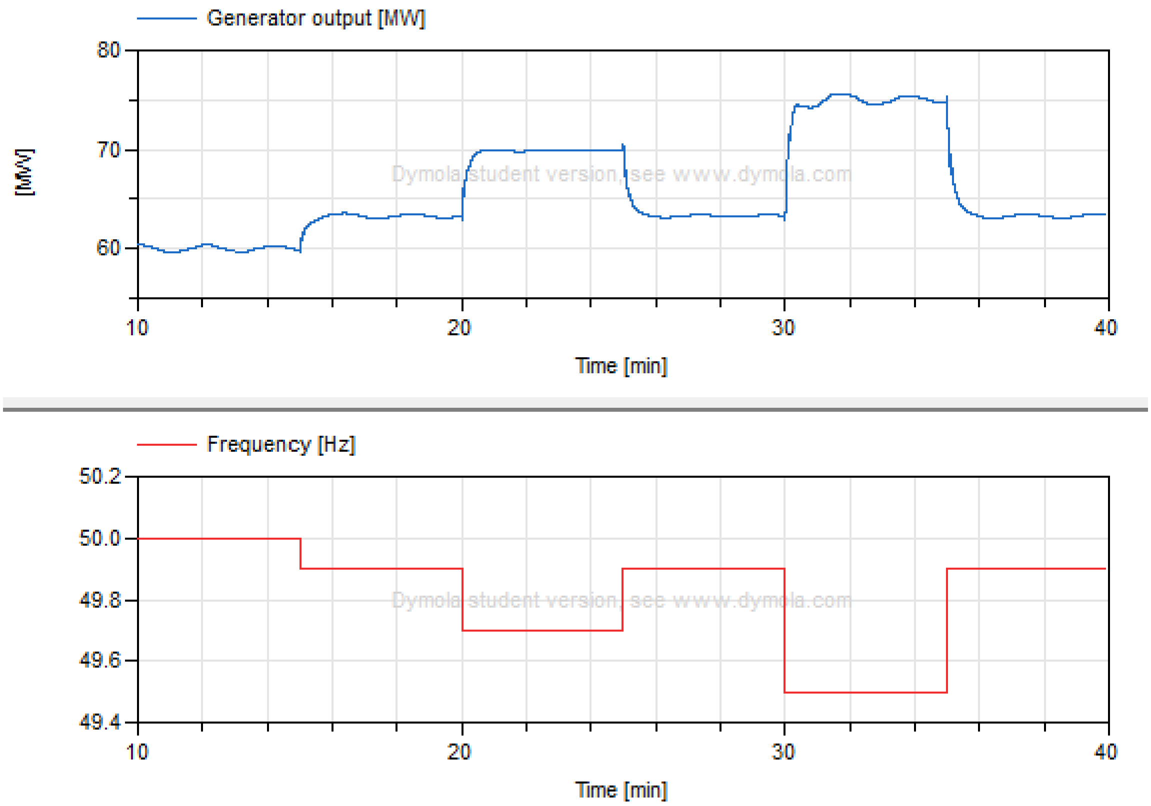

Figure 7.13: FCR-D upwards regulation step resonse at Hjartdøla poer plant

Table 7.12: FCR-D upwards step resonse at Hjartdøla poer plant

Frequency step $[Hz]$	$\Delta P\ [MW]$
50.0 - 49.9	3.2
49.9 - 49.7	6.6
49.7 - 49.9	6.6
49.9 - 49.5	13.2
49.9 - 50.0	13.2

The steady-state FCR-D activation is power response found from the frequency step change 49.9 - 49.5 Hz in table 7.12:

$$\Delta P_{ss} = 13.2MW \tag{7.16}$$

The ramp response is fond by applying a frequency input from 49.9 Hz to 49.0 Hz with a slope of -0.3 Hz/s.

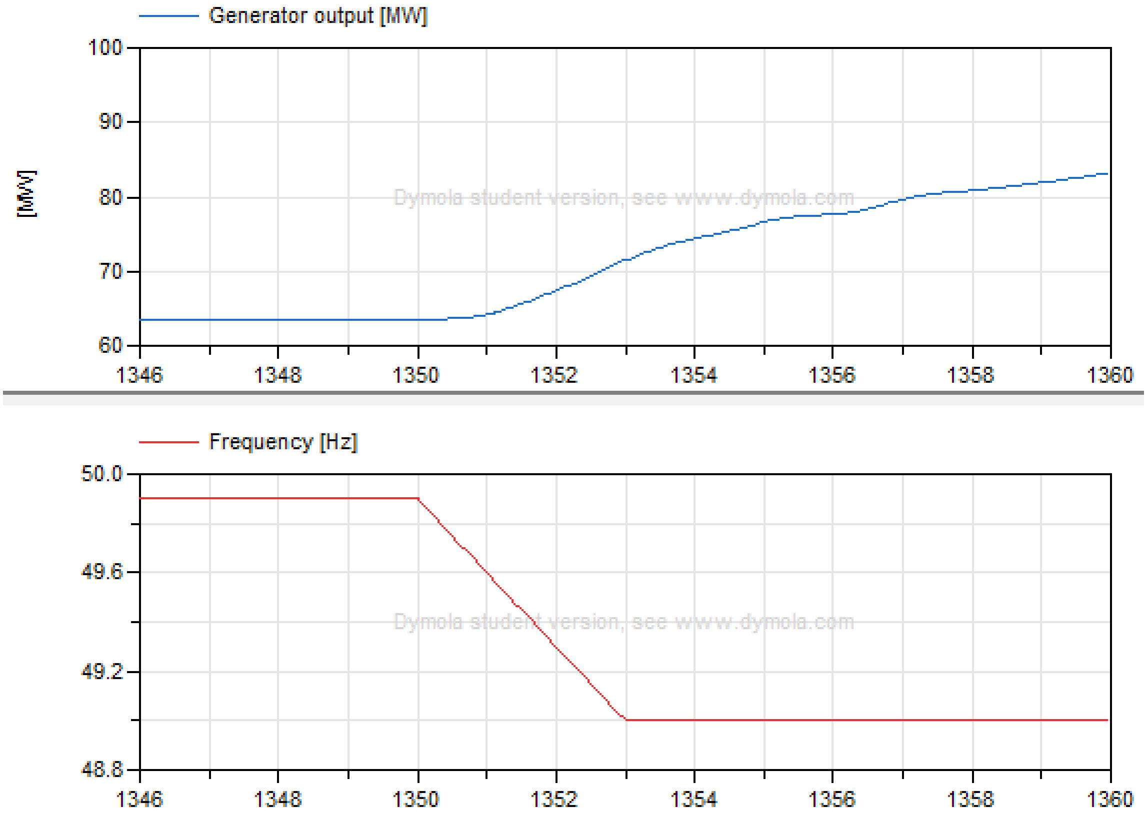

Figure 7.14: FCR-D ramp response at upward regulation for Hjartdøla power plant

The frequency ramp is applied to system at the time 1350 s. The activated power 5 seconds after the start of the ramp is:

$$\Delta P_{5s} = 12.8MW \tag{7.17}$$

and activated energy 5 seconds after the initiation of the ramp is:

$$E_{supplied} = 29.4MWs \tag{7.18}$$

Then, the FCR-D capacity at upwards regulation for Hjartdøla power plant is calculated:

$$C_{FCR-D_{up}} = \min(13.8, 13.2, 16.4) = 13.2MW \tag{7.19}$$

The FCR-D capacity is equal to the steady-state activated power, which means that the governor is fast enough to deliver å good performance five seconds after the start of the ramp.

To test the stability, the Nycuist curve given by the FCR-vectors multiplied with the grid transfer function $G_{FCR-D}(s)$ is plotted in the Nyquist diagram shows in figure 7.15.

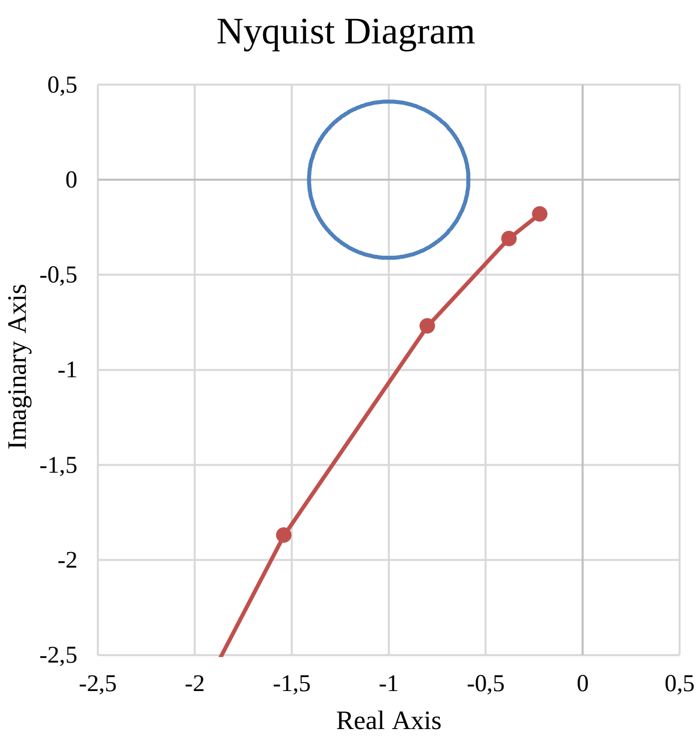

Figure 7.15: Nyquist Diagram for FCR-D upwards regulation at Hjartdøla power plant

From the Nyquist diagram the unit is qualified the stability requirements for FCR-D delivery at upwards regulation since the Nyquist curve does not enter the Nyquist point $(-1, 0j)$ as well as the stability margin circle.

7.2.4 FCR-D downward regulation

A frequency step sequence is applied to the governor in order to find the power response and determine the steady-state activation at downward regulation.

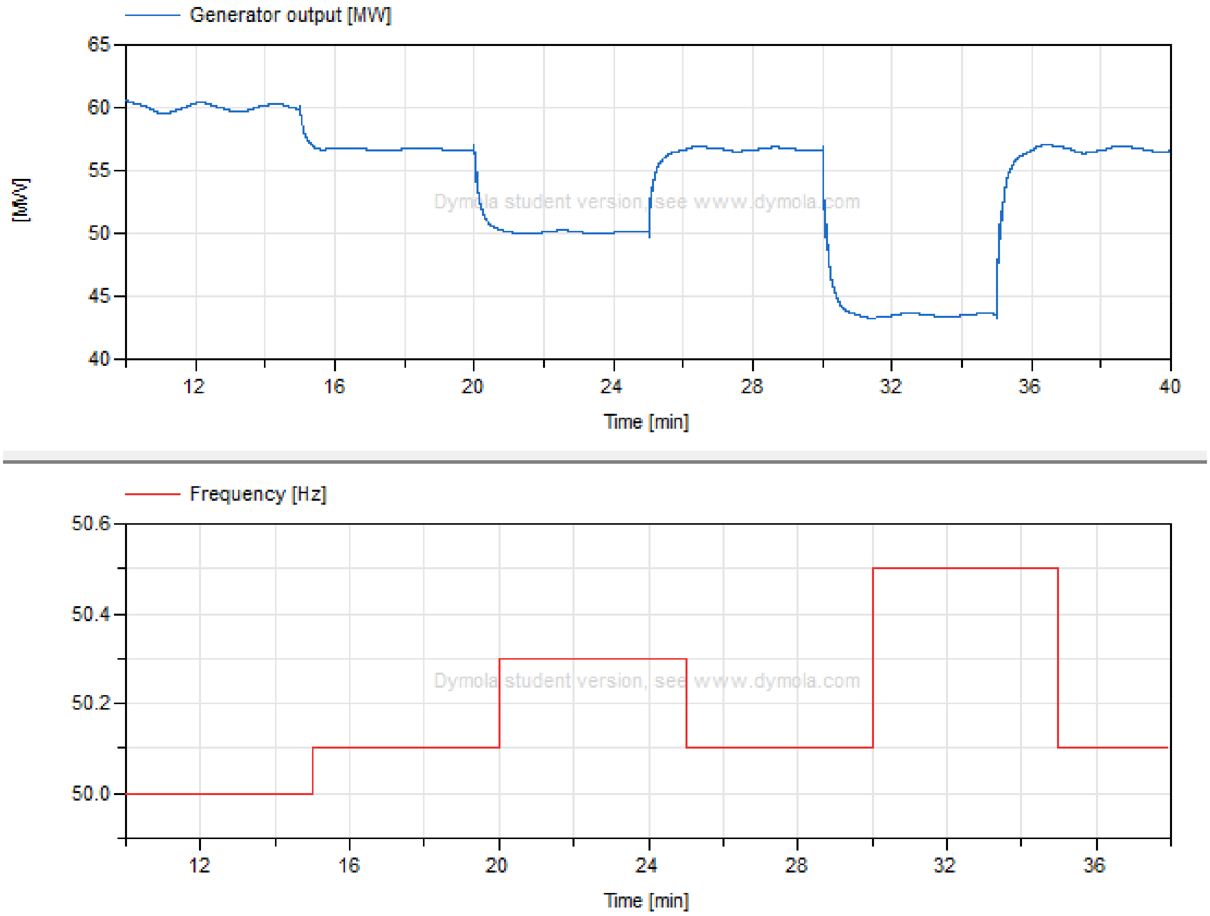

Figure 7.16: FCR-D downward step response for Hjartdøla power plant

Table 7.13: FCR-D downward step response for Hjartdøla power plant

Frequency $[Hz]$	$\Delta P\ [MW]$
50.0-50.1	3.3
50.1-50.3	6.6
50.3-50.1	6.6
50-150.5	13.2
50.1	13.2

From table 7.13, the steady-state activation for FCR-D downward regulation is:

$$\Delta P_{ss} = 13.2MW \tag{7.20}$$

In order to determine the active power and energy, and finally find the FCR-D capacity, a ramp response from 50.1 Hz to 51.1 Hz with a slope of 0.3 Hz/s is applied to the governor.

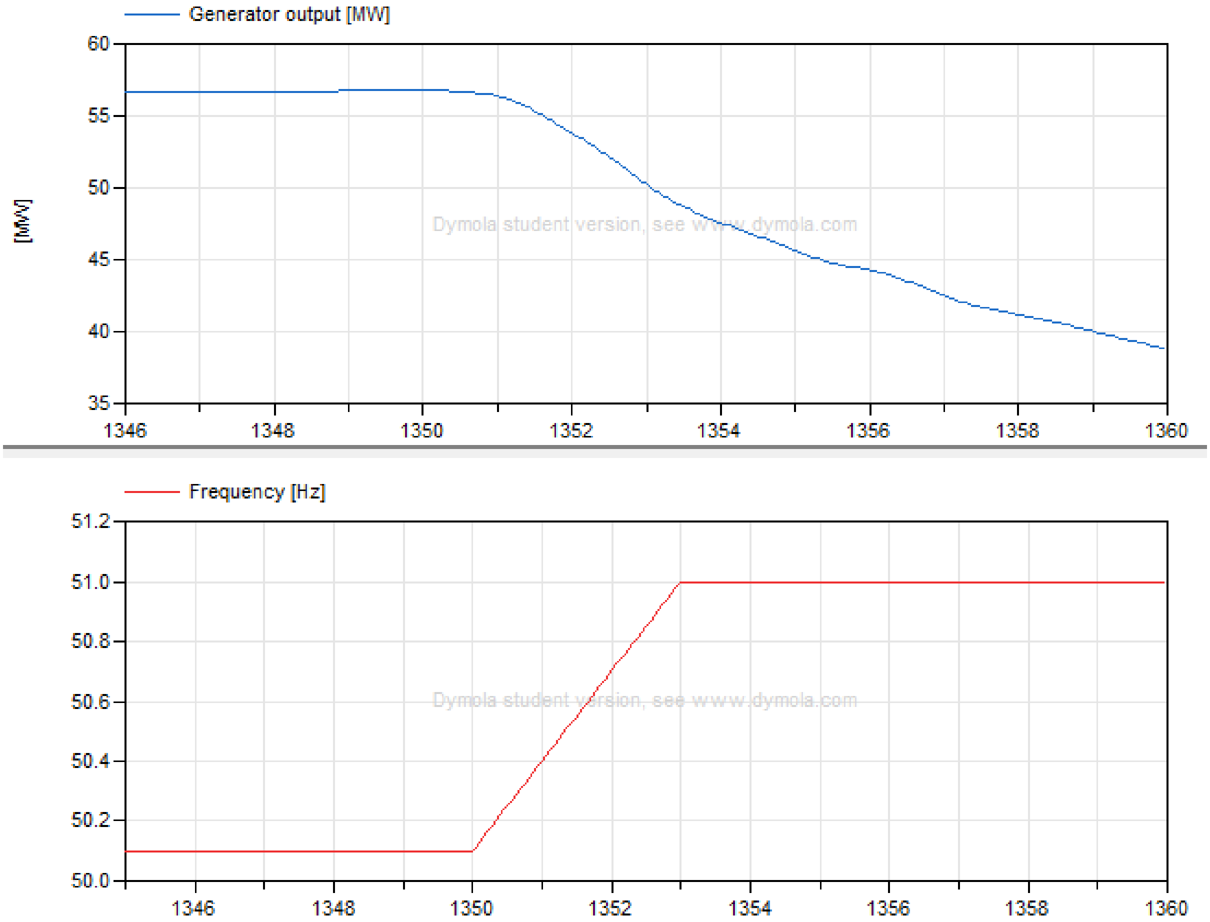

Figure 7.17: FCR-D ramp response at downward regulation for Hjartdøla power plant

The activated power and energy 5 seconds after start of the ramp is:

$$\Delta P_{5s} = 11.2MW \tag{7.21}$$

$$E_{supplied} = 31.7MWs \tag{7.22}$$

The FCR-D capacity is calculated by equation (4.5):

$$C_{FCR-D_{down}} = min(12.0, 13.2, 17.6) = 12.0MW \tag{7.23}$$

The FCR-D capacity at downwards regulation is a bit lower than the steady-state value. This means that the unit is unable to activate steady-state power response within 5 seconds.

Against, to plot the Nyquist curve in order to verify the stability requirement, the FCR-vectors is multiplied with the power system transfer function$G_{FCR-D}(s)$.

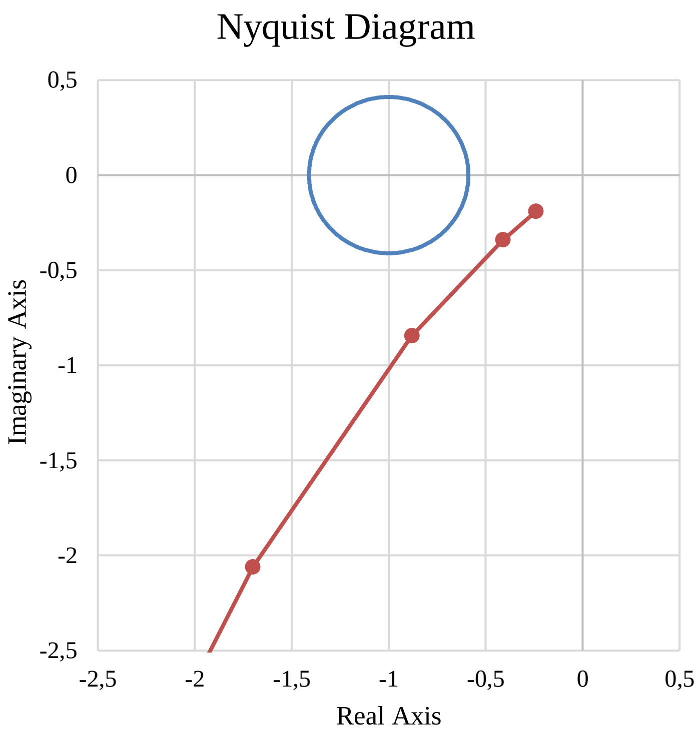

Figure 7.18: Nyqist Diagram Nyquist Diagram for FCR-D downwards regulation at Hjartdøla power plant

The scaling factor $\frac{\Delta P_{ss}}{C_{FCR-D}}$ is 1.1 for the FCR-D downwards regulation. Although the unit have lower capacity compared to its full steady-state activation, the hydropower unit fulfil the stability requirement for FCR-D delivery.

8 Discussion

8.1 Simulation models

The simulation models have been attempted to reflect the behaviour of the Sundsbarm and Hjartdøla power plants by using parameters found from technical documentation given by Skagerak Kraft As. However, some parameters are obtained from FIKS or calculated according to recommended dimensioning for stability.

The turbine governor has been attempted tuned by Skogestad's method using a simplified hydropower unit described by transfer functions. Skogestad is a way to find a good start for the PI-parameters and some uncertainty must be considered. In real, the turbine governor is delivered from the system supplier complete tuned, according to the requirements from FIKS. It is therefore difficult to recreate an identical model of the governor in the simulation model. Therefore, it is tested whether the parameters obtained from the Skogestad's method provide satisfactory phase margin and margin of requirement according to the FIKS. Both for Sundsbarm and Hjartdøla power plant, the PI parameters provide a little too much gain and phase margin in relation to the FIKS requirement. Stability analysis using Bode diagram is therefore used as a control to obtain correct proportional gain value and integrator gain value.

In the simulation model for both Sundsbarm and Hjartdøla power plant, the proportional gain value had to be reduced considerably, and the integrator gain value had also to be reduced slightly in order to obtain an asymptotic stable system almost equal to the behaviour in the commissioning report. This can probably be explained by the long simulation time of about 40 minutes and numbers of intervals set to 50 000.

It is of interest to look at the simulated steady-state power change when a frequency change is applied to the system compared with the theory using equation (3.15) about droop. Theoretically, the change in power of a generator can be expressed as:

$$\Delta P = -\frac{\Delta f/f_n}{R_i/P_{i,n}} \tag{8.1}$$

From equation (7.1), the theoretical value of steady-state FCR-N activation at the Sundsbarm power plant with 12% droop setting is $1.72\ MW$. This is consistent with simulated power change with an error of $0.01\ MW$. The small difference may be due to inaccurate reading of the simulation results. The simulated values in changes of FCR-D activated power for both Sundsbarm and Hjardøla is in accordance with the theoretical values, as well as the power change value for FCR-N for Hjardøla power plant. Overall, the calculated theoretical values give a correct estimate of how much primary control the hydropower unit in Sundsbarm and Hjartdøla power plant can deliver to the power system.

8.2 Stability and Performance

The FCR stability requirement is somewhat close to the existing requirement in the Norwegian way of setting the stability requirements. Today's requirements for frequency control in Norway are based on stability in separate operation while the new FCR-N/D requirements are developed to meet the Nordic demand for frequency quality/stability in synchronous operation. I.e. the 'system' that regulates against is different compared to today's FIKS requirements. This is also probably the reason why the stability analysis has a new step from Bode diagram to Nyquist diagram in order to enable tests the hydropower unit locally together with the Nordic power system.

As mentioned, the results of the tests for Sundsbarm power plant at minimum load with 4% droop setting and Hjartdøla power plant at minimum load with 12% droop setting is not present in the thesis. Because of different droop setting the results shows other power values, but apart from that, the behaviour is almost equal. The only difference between the results presented in chapter 7 is that the Nyquist curve does not enter the stability circle in some cases. However, it seems that the curves will pass on the right side of the circle and can be assumed as stable. However, shorter time periods could have been tested in order for the curve to pass the circle.

Results from the prequalification tests show that both the FCR-N and FCR-D stability requirements are fulfilled for Sundsbarm power plant as well as for Hjartdøla power plant. This can first be explained by the low waterway time constants. Short acceleration time of the water masses corresponds to short time in order to change the amount of produced power, which leads to better stability compared with long acceleration time. Therefore, low waterway time constant is crucial in order to achieve a stable system.

It has also been seen that backlash is crucial for whether the hydropower unit meets the requirements or not [31]. A backlash has shown to partly limit the ability of hydropower unit to contribute precise frequency control in normal operation. In a simulation model, it will probably be difficult to mirror the backlash that can perceive in a real plant. However, deadband can be implemented in the governor that will seem almost like backlash. As shown in the simulations for Sundsbarm and Hjartdøla power plant, no backlash exists. Therefore, this is not included in this thesis.

The requirements in FIKS say a lot about stability, but minimal about performance. This is a greater focus in the new FCR-N/D requirements in order to reduce the size of imbalance. There are no specific requirements for FCR-D delivery, but the unit shall deliver what it should within 5 seconds after a disturbance. With today's trends with lesser inertia in the system, it is necessary that the total amount of reserve is activated quickly to compensate for the inertia. The prequalification tests show that Sundsbarm and Hjartdøla power plants are able to deliver steady-state activation or almost steady-state activation within 5 seconds both at maximum and minimum droop settings. This is primally due to fast governors, but also because of low waterway time constants.

9 Conclusion

A set of prequalification tests, still under development, are performed on the simulation models of Sundsbarm and Hjartdøla power plants. The step response tests expose that the amount of FCR-N delivery from the hydropower unit in Sundsbarm is $1.72\ MW$ with 12% droop setting and $5.16\ MW$ with 4% droop setting. While the unit in Hjartdøla power plant can deliver $1.1\ MW$ with 12% droop setting and $3.3\ MW$ with 4% droop setting. The results from the simulations are accordance with the theory.

To decide the stability and dynamic performance of the units in synchronous operating, a set of sine test at different time periods was applied to the simulation models. At both the power plants, the units were shown to provide good dynamic performance for FCR-N delivery. The unit response together with the system response at different time periods was plotted in Nyquist diagram which showed that the stability is proved to be satisfactory at both Sundsbarm and Hjartdøla power plants. In some cases, it could be useful to test for shorter time periods to guarantee stability. Satisfactory stability is mainly due to the low water time constants and that the units have sufficient rotating masses relative to the waterway time constant.

Results from the FCR-D step and ramp response tests expose that the hydropower units can deliver 100% steady-state power response within 5 seconds. Except for the unit in Hjartdøla power plant with 4% droop setting which can deliver 91% of full steady-state response at downwards regulation.

References

[1] J. B. D. J. B. Jan Machowski, Power System Dynamic: Stability and Control, 2nd Edition, Wiley, 2008.

[2] Statnett, “Om reservemarkeder,” 7 April 2017. [Online]. Available: http://www.statnett.no/Kraftsystemet/Markedsinformasjon/. [Accessed 9 January 2018].

[3] M. K. M. L. A. I. B. E. A. J. A. D. K. E. N. M. Erik Ørum, “Future system inertia,” Entso-e.

[4] Statnett, “Systemdrifts- og markedsutviklingsplan 2017-2012,” 2017. [Online]. Available: http://www.statnett.no/Global/Dokumenter/Kraftsystemet/Systemansvar/Hoved_Systemdrift_N_lores_enkeltsider.pdf. [Accessed 15 January 2018].

[5] Statnett, «Forum for systemtjenester 2015,» October 2015. [Internett]. Available: http://www.statnett.no/Global/Drift%20og%20Marked/Forum%20for%20systemtjenester/Presentasjonspakke%20Dag%201%20Forum%20for%20Systemtjenester%202010 2015.pdf.

[6] Statnett, “Primærreserver (FCR),” 26 October 2017. [Online]. Available: http://www.statnett.no/Kraftsystemet/Markedsinformasjon/Primarreserver/. [Accessed 9 January 2018].

[7] L. v. d. S. Pieter Schavemaker, Electrical Power System Essentials, Wiley, 2009.

[8] Statnett, “Vilkår for tilbud, aksept, rapportering og avregning i marked for primærreserver til Statnett,” 19 Mars 2015. [Online]. Available: http://www.statnett.no/Global/Dokumenter/Kraftsystemet/Systemtjenester/Vilk%C3%A5r%20gjeldende%20fra%2019%20mars%202015.pdf. [Accessed 9 January 2018].

[9] Statnett, “Sekundærreserver (aFRR),” 20 December 2017. [Online]. Available: http://www.statnett.no/Kraftsystemet/Markedsinformasjon/sekundarreserver/. [Accessed 9 January 2018].

[10] Statnett, “Tertiærreserve (FRR-M),” 6 June 2016. [Online]. Available: http://www.statnett.no/Kraftsystemet/Markedsinformasjon/RKOM1/. [Accessed 9 January 2018].

[11] Svenska Kraftnät, Statnett, “The Nordic Balancing Concept,” June 2017. [Online]. Available: http://www.statnett.no/Global/Dokumenter/Kraftsystemet/Markedsinformasjon/Landssentralen/The%20Nordic%20Balancing%20Concept.pdf. [Accessed 4 January 2018].

[12] L. v. d. S. Pieter Schavemaker, Electrical Power System Essentials, John Wiley & Sons, 2008.

[13] Svenska Krafttnät, Statnett, “Presentation of renewed Nordic balancing,” [Online]. Available: http://www.statnett.no/Global/Dokumenter/Kraftsystemet/Markedsinformasjon/Landssentralen/Presentation%20of%20renewed%20Nordic%20balancing.pdf. [Accessed 5 January 2018].

[14] T. K. Nielsen, “Dynamisk dimensjonering av vannkraftverk,” SINTEF, Trondheim, 1990.

[15] V. Hveding, Vassbygging, Tapir forlag, 1978.

[16] A. Kjølle, Mechanical Equipment, Trondheim, 2001.

[17] S. J. Chapman, Electric Machinery Fundamentals, McGraw-Hill, 2012.

[18] G. J. Hegglid, *Lecture Power System Operation and Smart Grid - Frequency Control,* University College in Southeast Norway, 2018.

[19] Statnett SF, Funksjonskrav i kraftsystemet 2012.

[20] F. A. Haugen, Reguleringsteknikk, Fagbokforlaget, 2014.

[21] F. Haugen, “Control Theory,” [Online]. Available: https://home.usn.no/hansha/documents/control/theory/frequency_response.pdf. [Accessed 9 April 2018].

[22] T. A. B. A. F. Jens G. Balchen, Reguleringsteknikk, 2003.

[23] H.-P. Halvorsen, “Lectures: Frequency Response and Stability Analysis,” [Online]. Available: http://home.hit.no/~hansha/documents/control/lectures/Frequency%20Response%20and%20Stability%20Analysis.pdf.

[24] R. Eriksson, N. Modig og A. Westberg, «FCR-N Design og Requirements,» Entso-E, 2017.

[25] M. Kuivaniemi, N. Modig og R. Eriksson, «FCR-D Design of Requirements,» Entso-E, 2017.

[26] FCP project Prequalification Working Group, “Technical Requirements for Frequency Containment Reserve Provision in the Nordic Synchronous Area,” Enso-e, 2017.

[27] FCP project Prequalification Working Group, «Supporting Document on Technical Recuirements for Frequency Containment Reserve Provision in the Nordic Synchronous Area,» Entso-e, 2017.

[28] “Modelon,” [Online]. Available: http://www.modelon.com/products/modelon-library-suite/hydro-power-library/. [Accessed 8 Mars 2018].

[29] Statkraft , “Sundsbarm,” [Online]. Available: https://www.statkraft.no/Energikilder/vaare-kraftverk/norge/Sundsbarm/. [Accessed 16 February 2018].

[30] K. A. Rosvold, “Store norske leksikon,” 17 April 2013. [Online]. Available: https://snl.no/Hjartd%C3%B8la_kraftverk. [Accessed 19 March 2018].

[31] E. A. J. (. Evert Agneholm (DNV-GL), “FCP Project Summary report,” ENTSO-E, 2017.

Appendices

Appendix A: Task description

University College of Southeast Norway

Faculty of Technology, Natural Sciences and Maritime Sciences, Campus Porsgrunn

FMH606 Master's Thesis

Title: Frequency stability in integrated synchronous power systems

USN supervisor: Professor II Gunne J Hegglid

External partner: -

Task Background:
The frequency control of an interconnected power system is crucial to keep operational security of the system within specified limits simultaneously operate the power transmission and generation in an economical optimal way.

The Nordic synchronous system includes Finland, Sweden, Sealand of Denmark and Norway. The TSO of each of the countries are responsible for system balancing within each country. The balancing process' main activity is to keep power generation equal to the consumption every minute of day, night, week and year. If so, the network frequency, which is equal all over the synchronous system (which is the definition to such), will stay constant at 50.00 Hz. But impact from normal load variation, unwanted / unplanned generation and load outages and deviations in load and generation prognosis will lead to ever lasting unbalance and frequency variation. Especially the late years development of unregulated renewable generation capacity has caused decrease in quality of frequency control of the Nordic synchronous system.

The TSOs of the Nordic countries have ongoing comprehensive project work (FCP-project – Revision of the Nordic Frequency Containment Project) on increasing quality of frequency control. The TSO, have as activities within Entso-E, published a project phase 1 of their work and these documents will be the basis of this master thesis. (Entso-E is an EU-based organization of mainly the TSOs of countries within EU and associated member countries included Statnett of Norway.)

The development described in ongoing projects on system balancing executed by the Nordic TSOs may impact local control in power plants. This exercise will contain items within the existing and future regimes for system frequency control through reviewing of governing documents issued mainly by the TSOs. Study of existing local control and frequency control equipment and documentation thereof and simulation of dynamic behavior of these shall also be included.

Task description:

This master's thesis shall cover the following issues:

- Review of the existing supervision for frequency control given by FIKS 2012 – 'Funksjonskrav i kraftforsyningen' with weight on frequency control property requirements for hydropower units (HPU)

Address: Kjølnes ring 56, NO-3918 Porsgrunn, Norway. **Phone:** 35 57 50 00. **Fax:** 35 55 75 47.

- Describe the principle of todays balancing of the Nordic synchronous system and likewise the future MACE – Modernized Area Control Error-principle
- Review of the documents from the FCP-project with weight on which impact new regulation on frequency control may have on each single HPU control system
- Review the FCP-documents with respect to the specified test routines
- Do simulation of control performance of existing controllers for one or more of Skagerak Krafts HPUs with respect to the specified performance and test sequences

Student category: EPE students

Practical arrangements: -

Signatures:

Student (date and signature): 30.01.18 Sigrid Lauvik Lyngdal

Supervisor (date and signature): 30.1.2018 G J Hegglid

Appendix B: Turbine efficiency

Efficiency curve of the turbine at Sundsbarm power plant

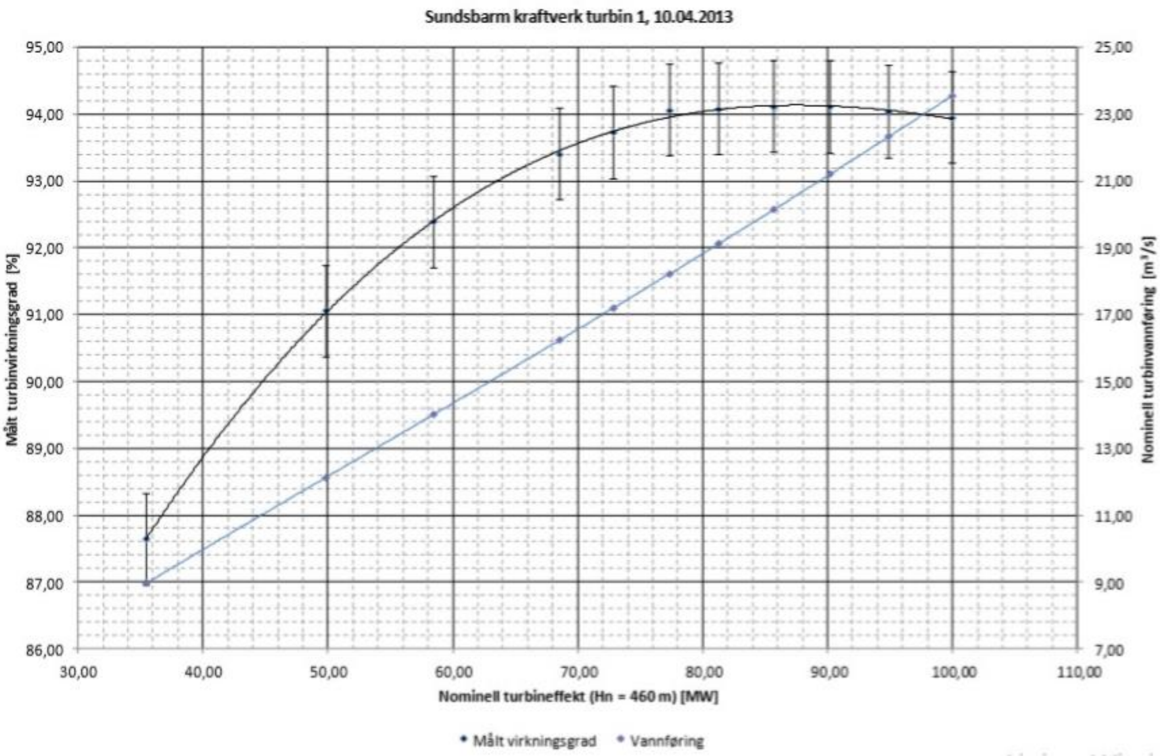

Efficiency of the turbine at Hjartdøla power plant

Effekter og vannf. omregnet til nom. fallhøyde, **555 m:**													
Turbineffekt	P_{Tn}	MW	26.96	36.96	43.77	51.63	58.53	65.42	47.15	32.91	28.28	23.55	18.71
Generatoreffekt	P_{Gn}	MW	26.12	36.09	42.89	50.70	57.55	64.37	46.25	32.05	27.43	22.72	17.93
Turbinvannføring	Q_{Tn}	m^3/s	5.52	7.50	8.87	10.48	11.92	13.40	9.56	6.74	5.76	4.79	3.81

Appendix C: Commissioning reports Turbine governor Sundsbarm power plant

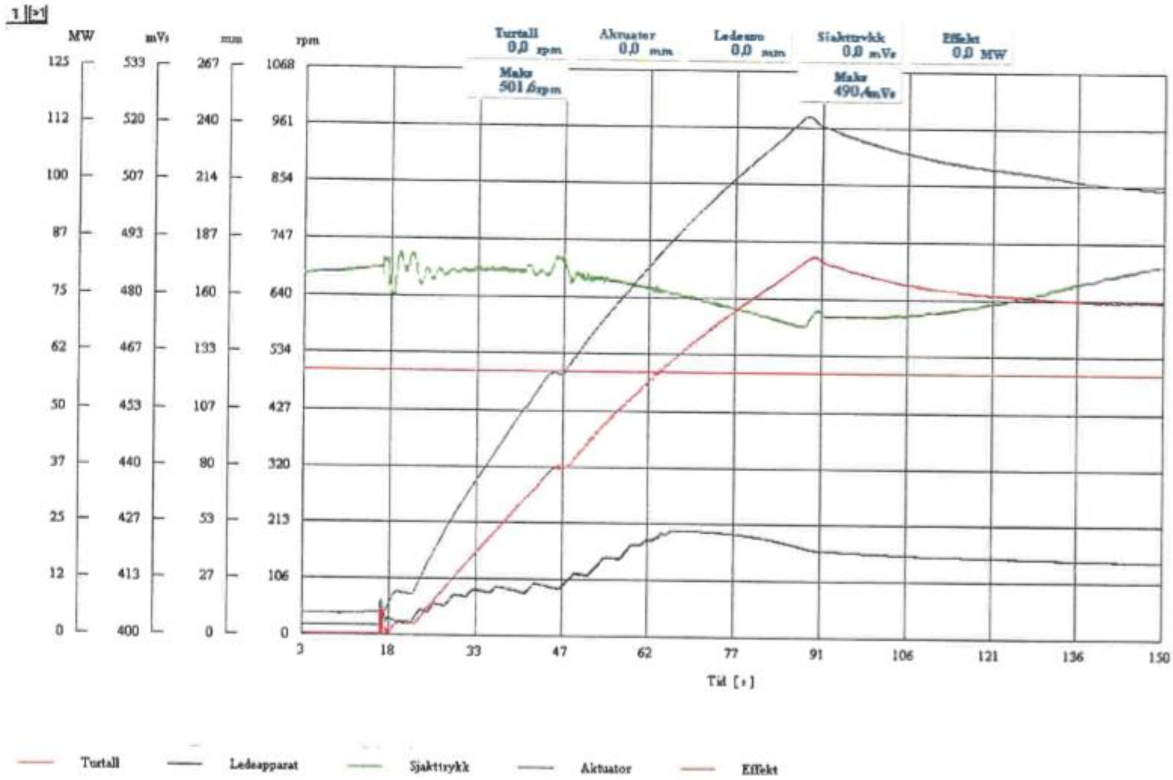

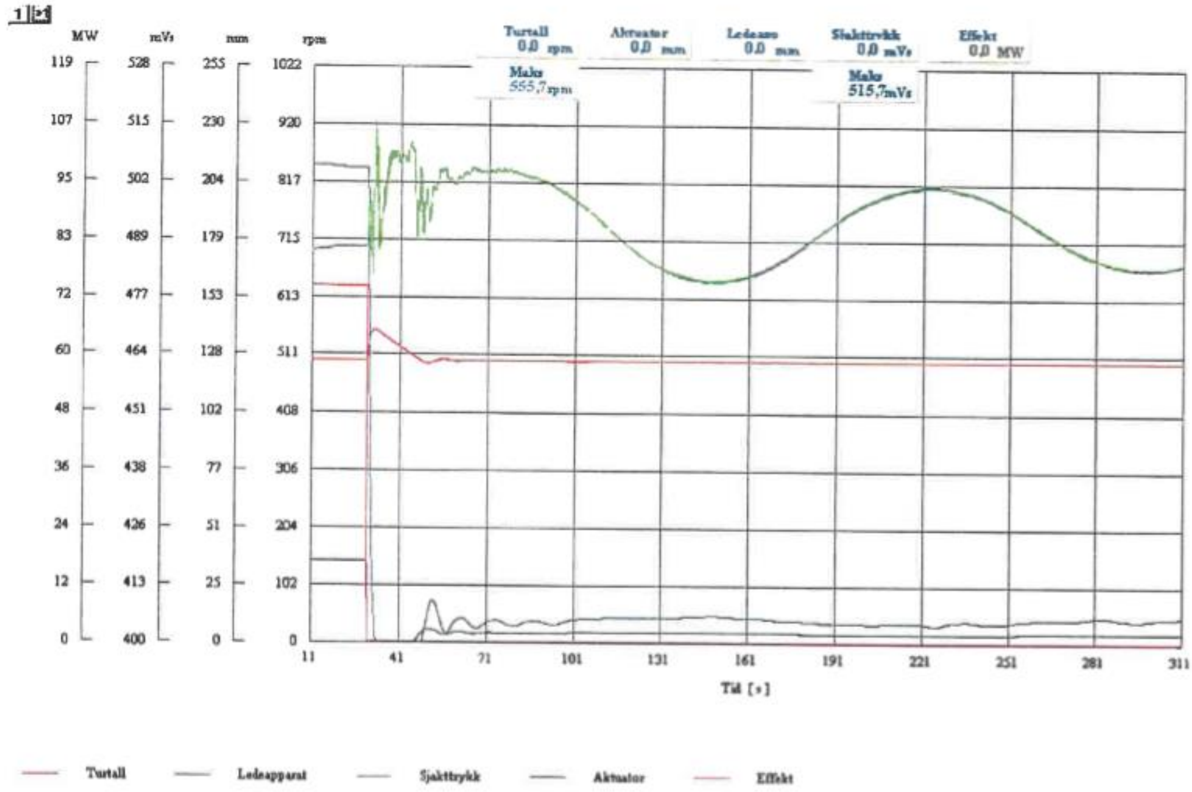

Vedlegg 5 Avslag 75 MW

Appendix D: Commissioning reports Turbine governor Hjartdøla power plant

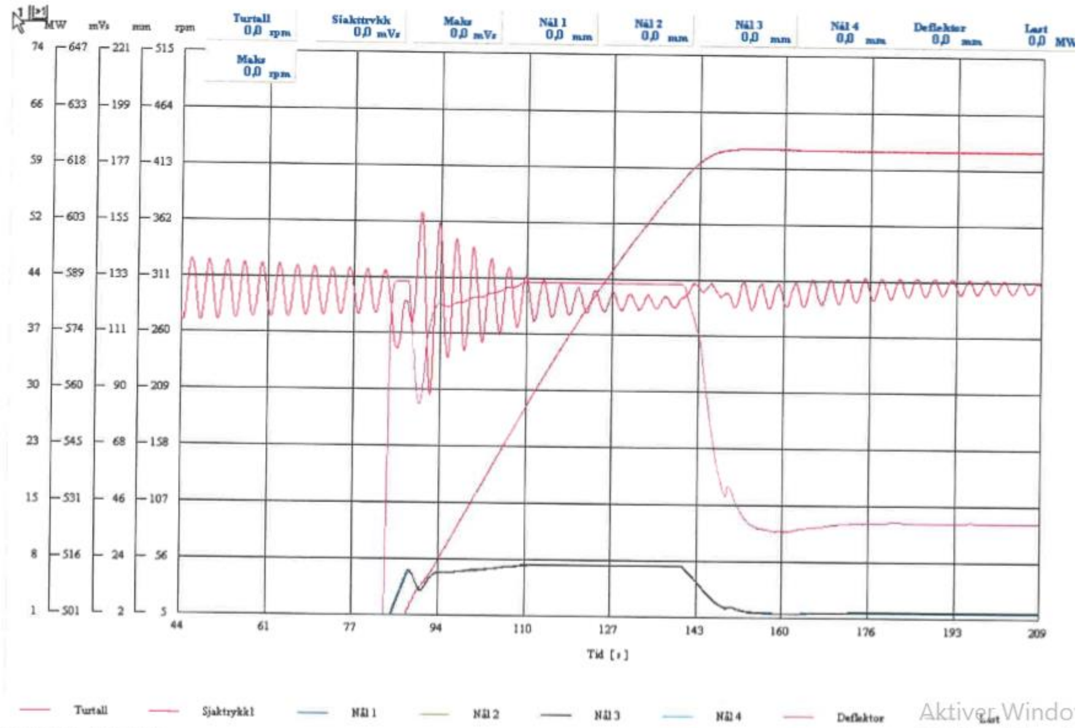

Vedlegg 2. Autostart

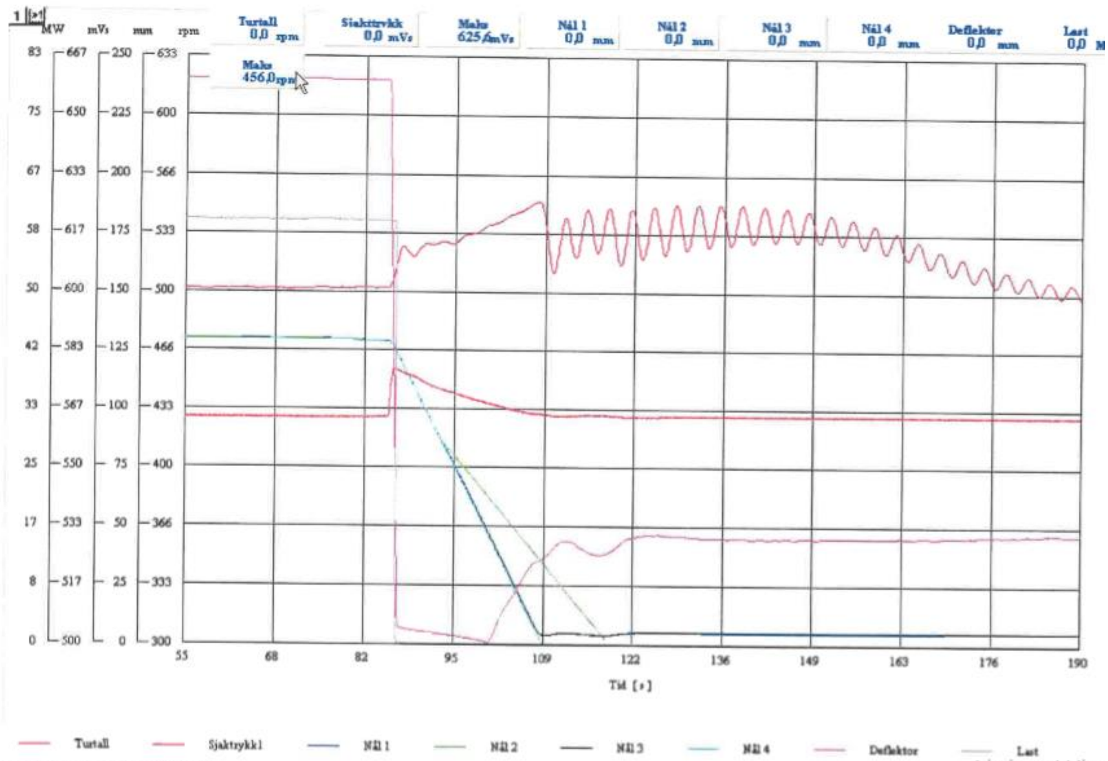

Vedlegg 6, avslag 60 MW

Appendix E: Results Sundsbarm power plant, minimum load

Results from Sundsbarm power plant at minimum load with 4% droop setting.

FCR-N dynamic performance

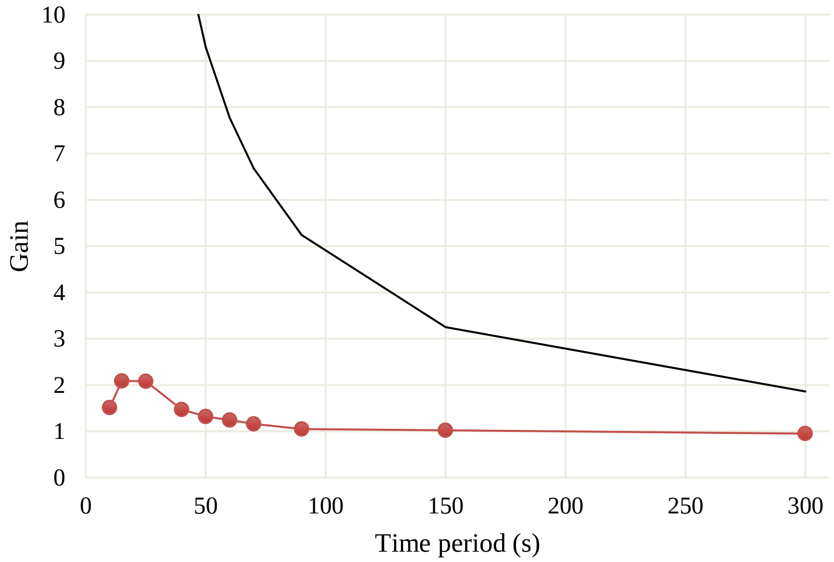

FCR-N dynamic performance requirement curve (black) together with the response curve (red)

FCR-N stability

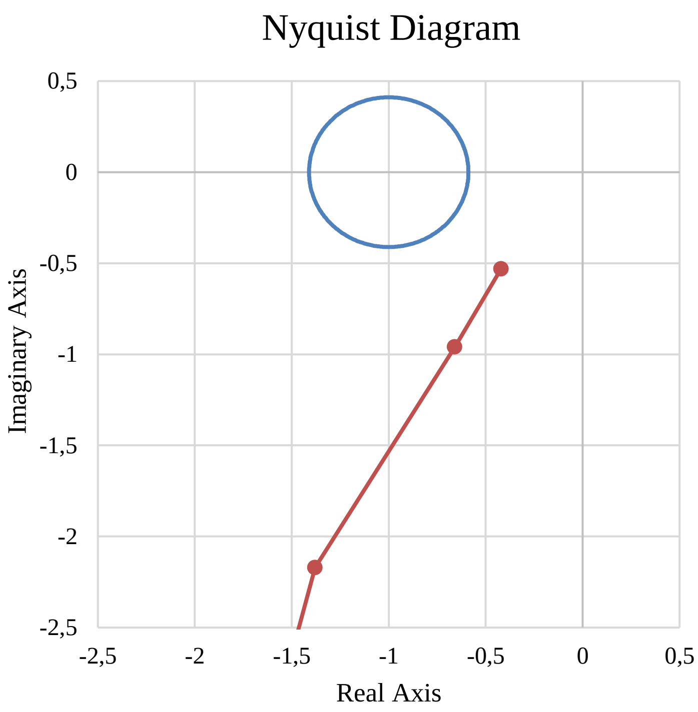

FCR-N stability requirement (blue) together with the response curve (red)

FCR-N stability for upwards regulation

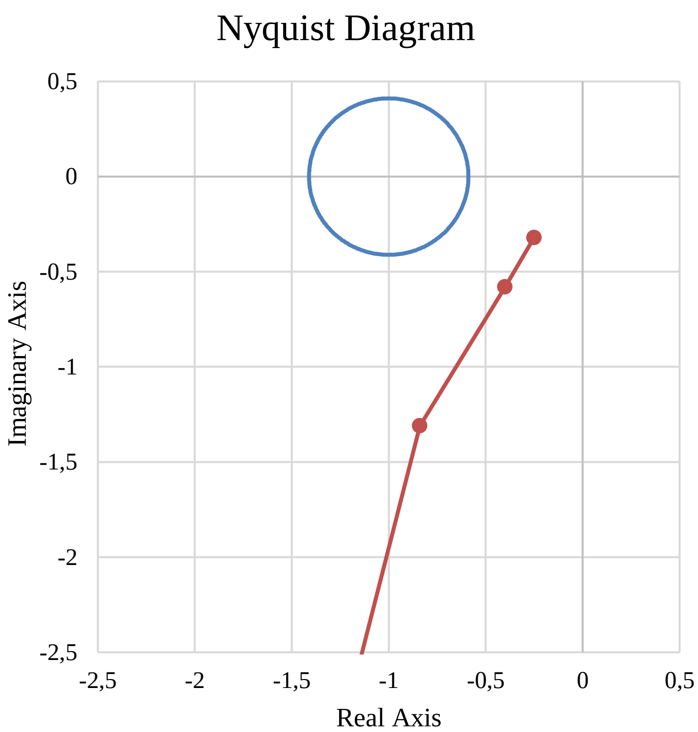

FCR-D stability requirement (blue) together with the response for upwards regulation (red)

FCR-N stability for downwards regulation

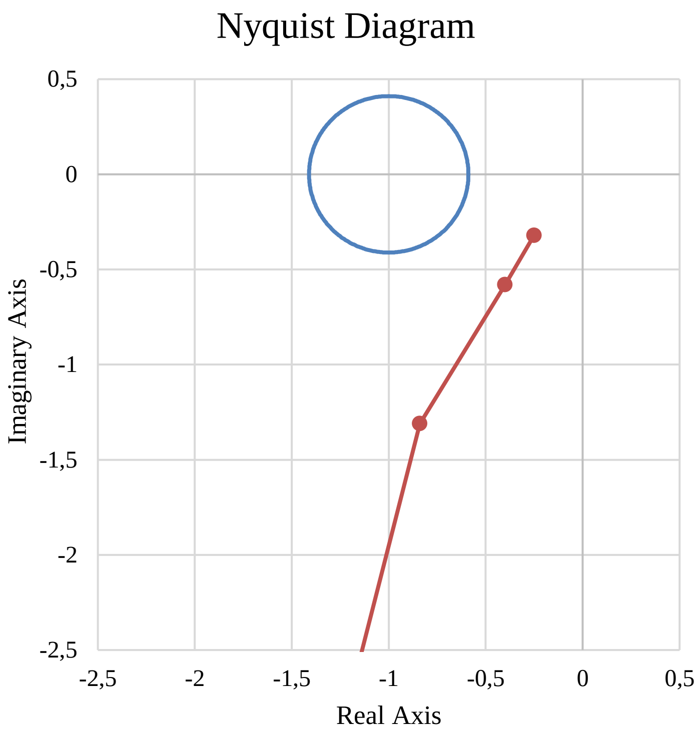

FCR-D stability requirement (blue) together with the response for downwards regulation (red)

Appendix F: Results Hjardøla power plant, minimum load

Results from Hjartdøla power plant at minimum load with 12% droop setting.

FCR-N dynamic performance

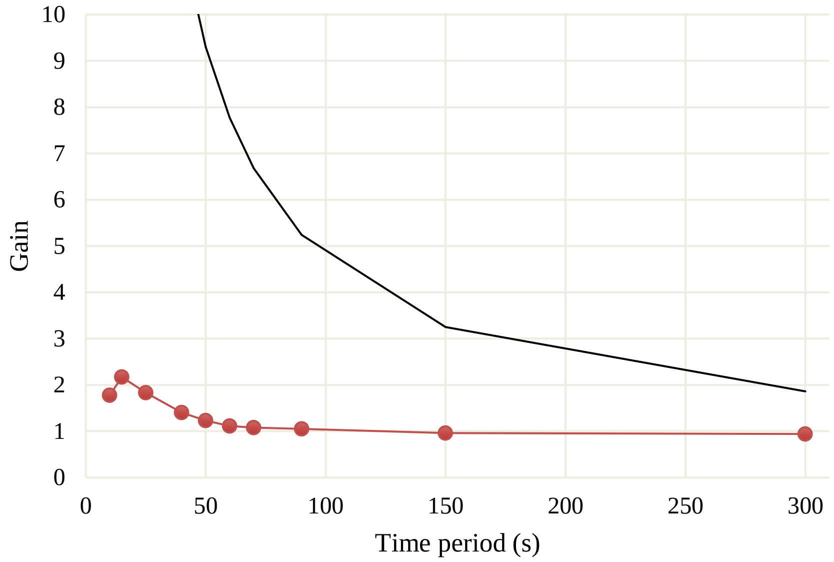

FCR-N dynamic performance requirement curve (black) together with the response curve (red)

FCR-N stability

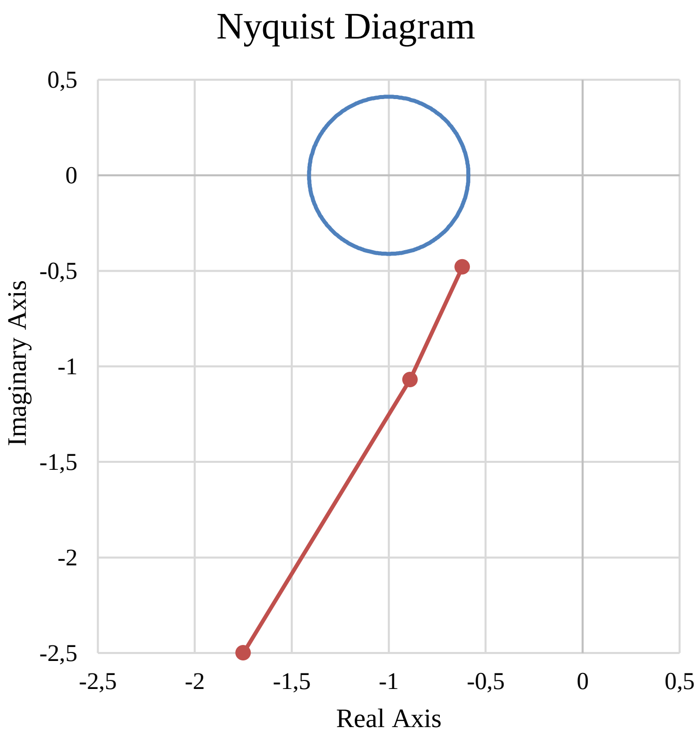

FCR-N stability requirement (blue) together with the response curve (red)

FCR-D stability for upwards reguation

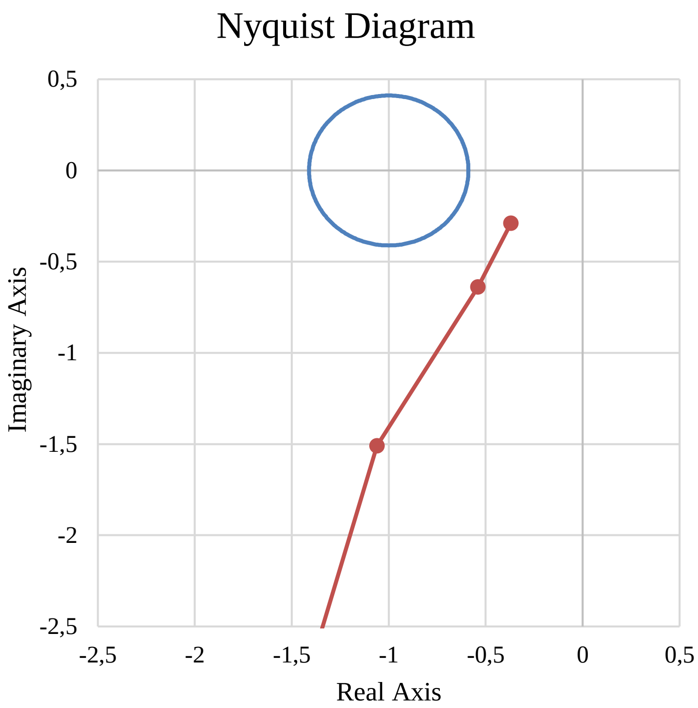

FCR-D stability requirement (blue) together with the response for upwards regulation (red)

FCR-D stability downwards reguation

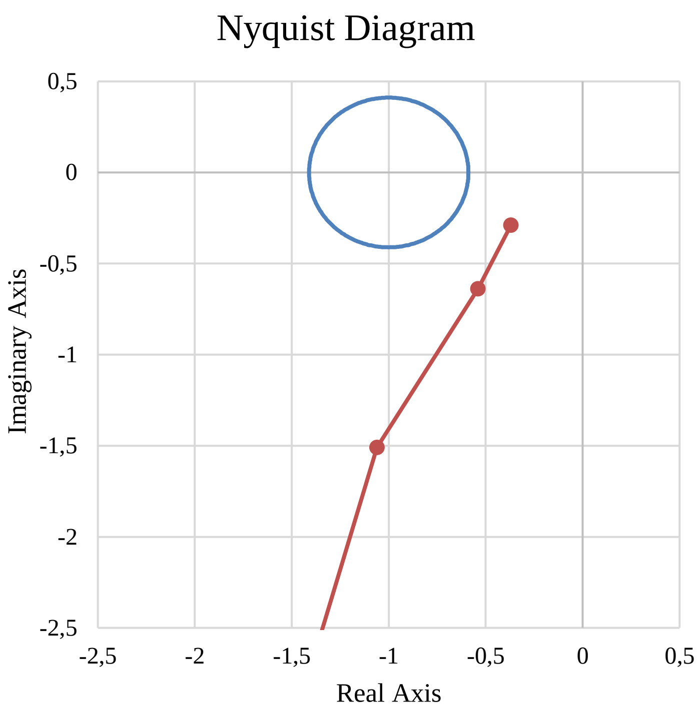

FCR-D stability requirement (blue) together with the response for downwards regulation (red)